NACA TN 2736 6606

TECH LIBRARY KAFB, NM
0065778

NATIONAL ADVISORY COMMITTEE FOR AERONAUTICS

TECHNICAL NOTE 2736

TWO-DIMENSIONAL SHEAR FLOW IN A 90° ELBOW

By James J. Kramer and John D. Stanitz

Lewis Flight Propulsion Laboratory
Cleveland, Ohio

Washington

June 1952

AFMDC
TECHNICAL LIBRARY
AFL 2811

TECH LIBRARY KAFB, NM
0065778

NATIONAL ADVISORY COMMITTEE FOR AERONAUTICS

TECHNICAL NOTE 2736

TWO-DIMENSIONAL SHEAR FLOW IN A 90° ELBOW

By James J. Kramer and John D. Stanitz

SUMMARY

As part of an approach to a better understanding of the motion of real fluids in flow machinery, two-dimensional, incompressible, nonviscous shear flows in a 90° elbow have been investigated. Solutions are presented for linear and sinusoidal velocity distributions across the inlet of the elbow. The solutions with linear inlet velocity distributions indicate that as the negative vorticity of the flow increased: (1) the static-pressure drop through the elbow decreased, (2) the local deceleration along the outer channel walls increased, and (3) the magnitude of the velocities on the channel walls changed greatly, but the local pressure coefficient rose only gradually and the difference in pressure coefficient at corresponding points on the two walls was practically unchanged. In the case of a sinusoidal inlet velocity distribution local decelerations occurred on both walls.

INTRODUCTION

As part of an approach to a better understanding of the motion of real fluids in flow machinery, two-dimensional, incompressible, nonviscous shear flows in a 90° elbow have been investigated at the NACA Lewis laboratory. For real, viscous fluids the velocity distribution upstream of the elbow is nonuniform and therefore the fluid motion is rotational. Such rotational, or shear, flows can develop both normal to and in the plane of the elbow. If the shear flow develops normal to the plane, so that the vorticity vectors are parallel to the plane, three-dimensional secondary flows develop in the elbow (references 1 to 3). If, however, the shear flow develops in the plane of the elbow, so that the vorticity vectors are normal to the plane, the shear flow remains two-dimensional and in the plane of the elbow. It is this latter two-dimensional shear flow that is investigated in this report. The purpose of the investigation is to determine the effects of this type of shear flow on the velocity and pressure distributions in a 90° elbow.

Two-dimensional potential solutions for irrotational flow in channels are well known (references 4 and 5, for example), and solutions for

two-dimensional shear flow about isolated bodies have been obtained (references 6 and 7, for example), but no solutions are known for two-dimensional shear flow in channels. In this report such solutions are presented for incompressible flow in a 90° elbow.

Although the shear flow is considered to have been generated by viscous forces acting on the fluid upstream of the region of turning, it is assumed that in the immediate vicinity of the region of turning, where the solutions are obtained, the viscous forces are small and can be neglected. Solutions are obtained for two types of velocity distribution upstream of the region of turning: linear and sinusoidal distributions. The streamlines and the velocity and pressure distributions of these solutions are compared with those of the potential solution from reference 8.

METHOD OF ANALYSIS

The differential equation for the distribution of shear flow in any two-dimensional channel is developed from Bernoulli's equation, and from the equations of motion and continuity. The flow is assumed to be incompressible and nonviscous.

Equations of motion. - The equations of motion are

$$-\frac{g}{\rho}\frac{\partial p}{\partial x} = u\frac{\partial u}{\partial x} + v\frac{\partial u}{\partial y} \tag{1a}$$

$$-\frac{g}{\rho}\frac{\partial p}{\partial y} = u\frac{\partial v}{\partial x} + v\frac{\partial v}{\partial y} \tag{1b}$$

where g is the acceleration due to gravity; ρ, the fluid weight density; p, the static pressure; x and y, Cartesian coordinates; and u and v, the velocity components in the x- and y-directions, respectively. All symbols are defined in appendix A. All variables are made dimensionless by expressing them as ratios of characteristic quantities in the following manner:

$$P = \frac{p}{\left[\frac{\rho(q_{e,av})^2}{2g}\right]} \tag{1c}$$

where $q_{e,av}$ is the arithmetic average of the resultant velocity q across the channel exit, downstream at infinity.

$$\left.\begin{aligned} U &= \frac{u}{q_{e,av}} \\ V &= \frac{v}{q_{e,av}} \\ X &= \frac{x}{w_e} \\ Y &= \frac{y}{w_e} \end{aligned}\right\} \tag{1d}$$

where w_e is the width of the channel at the exit.

After division by $\frac{(q_{e,av})^2}{2w_e}$, equations (1a) and (1b) become in dimensionless form

$$-\frac{\partial P}{\partial X} = 2U\frac{\partial U}{\partial X} + 2V\frac{\partial U}{\partial Y} \tag{2a}$$

$$-\frac{\partial P}{\partial Y} = 2U\frac{\partial V}{\partial X} + 2V\frac{\partial V}{\partial Y} \tag{2b}$$

Bernoulli's equation. - Bernoulli's equation states

$$\frac{p}{\rho} + \frac{q^2}{2g} = h \tag{3}$$

where h is the Bernoulli constant (constant along a streamline). The Bernoulli constant is made dimensionless by expressing it as a ratio of h to $\left[\frac{(q_{e,av})^2}{2g}\right]$ and the velocity is expressed nondimensionally as a ratio of q to $q_{e,av}$. Thus,

$$H = \frac{h}{\left[\frac{(q_{e,av})^2}{2g}\right]} \tag{3a}$$

$$Q = \frac{q}{q_{e,av}} \tag{3b}$$

Equation (3), having been divided by $\frac{(q_{e,av})^2}{2g}$, becomes, in nondimensional form,

$$P + Q^2 = H \tag{4}$$

Continuity equation. - The continuity equation in dimensionless form becomes

$$\frac{\partial U}{\partial X} + \frac{\partial V}{\partial Y} = 0 \tag{5}$$

Equation (5) is satisfied by a stream function Ψ, which is defined by the following relations

$$\left.\begin{aligned} \frac{\partial \Psi}{\partial X} &= -V \\ \frac{\partial \Psi}{\partial Y} &= U \end{aligned}\right\} \tag{6a}$$

Also, from equation (6a), in the direction of N

$$\frac{d\Psi}{dN} = Q \tag{6b}$$

where N is distance (dimensionless, expressed as ratio of w_e) along the outer normal to a streamline.

Differential equation. - From equation (4) with Q^2 written as $U^2 + V^2$

$$\frac{\partial P}{\partial X} + 2U\frac{\partial U}{\partial X} + 2V\frac{\partial V}{\partial X} = \frac{\partial H}{\partial X} \tag{7a}$$

$$\frac{\partial P}{\partial Y} + 2U\frac{\partial U}{\partial Y} + 2V\frac{\partial V}{\partial Y} = \frac{\partial H}{\partial Y} \tag{7b}$$

From equations (2a) and (7a)

$$2V\left(\frac{\partial V}{\partial X} - \frac{\partial U}{\partial Y}\right) = \frac{\partial H}{\partial X} \tag{8a}$$

and, similarly, from equations (2b) and (7b)

$$2U\left(\frac{\partial V}{\partial X} - \frac{\partial U}{\partial Y}\right) = -\frac{\partial H}{\partial Y} \tag{8b}$$

Because H is a function of Ψ only,

$$\frac{\partial H}{\partial X} = \frac{\partial \Psi}{\partial X}\frac{dH}{d\Psi} = -V\frac{dH}{d\Psi} \tag{9a}$$

and

$$\frac{\partial H}{\partial Y} = \frac{\partial \Psi}{\partial Y}\frac{dH}{d\Psi} = U\frac{dH}{d\Psi} \tag{9b}$$

From equations (6a), (8a), and (9a)

$$\frac{\partial^2 \Psi}{\partial X^2} + \frac{\partial^2 \Psi}{\partial Y^2} = \frac{1}{2}\frac{dH}{d\Psi} \tag{10}$$

Equation (10) is the differential equation for the distribution of the stream function in a two-dimensional channel with shear flow. Equation (10) can also be derived from equations (6a), (8b), and (9b).

Vorticity. - The vorticity ζ of the shear flow is defined by

$$\zeta = \frac{\partial V}{\partial X} - \frac{\partial U}{\partial Y} \tag{11}$$

which from equation (6a) becomes

$$\zeta = -\left(\frac{\partial^2 \Psi}{\partial X^2} + \frac{\partial^2 \Psi}{\partial Y^2}\right)$$

Thus, from equation (10) the vorticity is equal to $-\frac{1}{2}\frac{dH}{d\Psi}$, which is constant along streamlines so that

$$\zeta = -\frac{1}{2}\frac{dH}{d\Psi} = -\frac{1}{2}\left(\frac{dH}{d\Psi}\right)_i \tag{11a}$$

But, because the flow is parallel at the inlet,

$$\left(\frac{dH}{d\Psi}\right)_i = \left(\frac{dH}{dN}\right)_i \left(\frac{dN}{d\Psi}\right)_i$$

and from equation (4) with P_i constant

$$2Q_i \left(\frac{dQ}{dN}\right)_i = \left(\frac{dH}{dN}\right)_i$$

so that, after introduction of equation (6b), equation (11a) becomes

$$\zeta = -\left(\frac{dQ}{dN}\right)_i \tag{11b}$$

Therefore, the vorticity at a point on a streamline anywhere in the flow field can be determined by equation (11b) from the velocity gradient normal to the streamline at the inlet.

METHOD OF SOLUTION

The differential equation (10) was solved by relaxation methods for the examples of this report. In order to facilitate the solutions, the flow field in the XY-plane was transformed onto a field the coordinates of which are the streamlines and velocity potential lines for irrotational flow.

Transformation of coordinates. - For irrotational flow the stream function and velocity potential, η and ξ respectively, are defined by

$$\left.\begin{aligned} \frac{\partial \xi}{\partial X} &= \frac{\partial \eta}{\partial Y} = U_o \\ \frac{\partial \xi}{\partial Y} &= -\frac{\partial \eta}{\partial X} = V_o \end{aligned}\right\} \tag{12a}$$

where the subscript o indicates irrotational flow. Also, from equation (12a), in the direction of N_o and S_o

$$\frac{d\xi}{dS_o} = \frac{d\eta}{dN_o} = Q_o \tag{12b}$$

where Q_o is the resultant velocity for irrotational flow and where S is the distance (dimensionless, expressed as ratio of w_e) along streamlines. From equation (12b), if η is zero along the right channel wall when faced in the direction of flow, η is 1.0 along the left wall (because Q_o and ΔN are 1.0 at the exit of the channel, downstream at infinity). Thus, because ξ extends from minus to plus infinity, the flow field in the $\xi\eta$-plane is an infinite strip of unit width.

Differential equation. - The differential equation (10) transformed onto the $\xi\eta$-plane becomes (appendix B)

$$\frac{\partial^2 \Psi}{\partial \xi^2} + \frac{\partial^2 \Psi}{\partial \eta^2} = \frac{1}{2Q_o{}^2} \frac{dH}{d\Psi} \tag{13}$$

Velocity components. - The velocity Q and its components Q_ξ and Q_η in the ξ and η directions, respectively, are obtained from the distribution of Ψ by (appendix C)

$$Q = \sqrt{Q_\xi{}^2 + Q_\eta{}^2} \tag{14a}$$

where

$$Q_\xi = Q_o \frac{\partial \Psi}{\partial \eta} \tag{14b}$$

$$Q_\eta = -Q_o \frac{\partial \Psi}{\partial \xi} \tag{14c}$$

The velocity components U and V are related to Q_ξ and Q_η by (appendix C and fig. 1)

$$\left.\begin{aligned} U &= Q_\xi \cos \theta_o - Q_\eta \sin \theta_o \\ V &= Q_\xi \sin \theta_o + Q_\eta \cos \theta_o \end{aligned}\right\} \tag{15}$$

where θ_o is the local direction for irrotational flow (fig. 1).

Boundary conditions. - The stream function Ψ is constant along each of the channel walls. If Ψ is zero along the right wall ($\eta = 0$), then Ψ is 1.0 along the left wall ($\eta = 1.0$), because from equation (6b) and from the definition of Q

$$\Delta\Psi = \int_0^{1.0} Q \, dN = 1.0$$

across the channel at the exit downstream at infinity.

In theory the flow field extends to $\pm\infty$ in the direction of ξ. In practice, however, the relaxation solutions converge to essentially uniform flow conditions within a reasonably short distance from the region of turning.

Relaxation solutions. - The numerical examples were solved in the $\xi\eta$-plane by relaxation methods (references 4 and 9). A square grid with a spacing of 1/8 was used. The first example was solved using a three-point system for computing the derivatives, and the value of Ψ at each grid point was relaxed to a unit change in the fifth place. The second example was solved using a five-point system for computing the derivatives and the value of Ψ at each grid point was relaxed to a unit change in the fourth place. An investigation of the errors involved in the two methods of approximation to the derivatives showed comparable accuracy for the two solutions.

NUMERICAL EXAMPLES

The channel investigated by the two numerical examples in this report is the 90° elbow (89.36°) of reference 8. The elbow was designed in reference 8 for incompressible, potential flow with a prescribed velocity distribution that has no local decelerations along the channel walls. The transformed coordinates ξ,η and the values of Q_o required for the solution of equation (13) are tabulated in reference 8.

Numerical Example I

Inlet velocity distribution. - In example I a linear distribution of velocity across the inlet was prescribed such that the velocity Q varied from 0.25 on the inner wall (wall with smaller radius of curvature and at which η is 0) to 0.75 on the outer wall (η equals 1.0). (See fig. 2.) Thus,

$$Q_i = 0.25 + 0.50\,\eta_i \tag{16a}$$

For this inlet velocity distribution the distribution of H is (appendix D)

$$H = H_o + \frac{\Psi}{2} \tag{16b}$$

where H_o is the arbitrary value of H along the inner wall. Therefore, the vorticity of the shear flow becomes

$$\zeta = -\frac{1}{2}\frac{dH}{d\Psi} = -\frac{1}{4} \tag{16c}$$

so that for a linear inlet velocity distribution the vorticity is everywhere constant (and negative) in the channel. Also, for the linear inlet velocity distribution given by equation (16a) it can be shown that (appendix D)

$$\Psi_i = 0.5\,(\eta_i + \eta_i^2) \tag{16d}$$

$$\Psi_e = 0.875\,\eta_e + 0.125\,\eta_e^2 \tag{16e}$$

and

$$Q_e = 0.875 + 0.25\,\eta_e \tag{16f}$$

The exit velocity distribution is compared with the inlet distribution in figure 2.

Streamlines. - In figure 3 the streamlines for the shear flow of example I are presented in the physical XY-plane with the ξ,η grid system superposed. The spacing of the streamlines decreases linearly at both inlet and exit, indicating a linearly increasing variation in velocity at both positions, because the spacing of the streamlines is inversely proportional to the velocity. The velocity is more nearly uniform at the exit and, therefore, at the exit the streamlines Ψ of the shear flow are closer to the streamlines η of the potential flow than at the inlet.

Velocity distribution. - Lines of constant resultant velocity Q are presented in figure 4. The velocity component Q_η normal to potential flow streamlines is shown in figure 5. This velocity component is relatively small throughout the channel and disappears upstream and downstream of the region of turning and along the channel walls. Two points of relative maximum occur. These points are explained as follows. From figure 1

$$Q_\eta = Q \sin (\theta - \theta_o) \tag{17}$$

so that relative maximums for Q_η occur when the product of Q and $\sin (\theta - \theta_o)$ is maximum. The first maximum occurs in a region ($\eta \approx 0.375$, $\xi \approx 0.625$) where $(\theta - \theta_o)$ is large (fig. 3) and the second maximum occurs in a region ($\eta \approx 0.5$, $\xi \approx 2.75$) where Q is large.

The velocities along the inner and outer walls are plotted against ξ in figure 6 for example I and for the potential flow. The gradients of the velocity distributions for the two types of flow are similar. However, the magnitudes of the velocity are different. On the outer wall the velocities for example I are higher than for the potential flow solution, whereas on the inner wall the velocities for example I are lower. These velocity distributions result from the prescribed inlet velocity distribution which, as indicated by equation (11b), prescribes the vorticity throughout the channel. Thus the circulation around any closed path, which circulation is zero for potential flow, is equal to ζA, where A is the area of the region enclosed by the path. This expression for the circulation comes directly from Stokes' theorem and equations (5) and (11). Although no local decelerations occur along the channel walls for the potential flow, a slight deceleration occurs along the outer wall for the shear flow, example I.

The pressure coefficient along the inner and outer walls for example I and for the potential flow are presented in figure 7. The pressure coefficient is defined as

$$\frac{p - p_1}{\left[\frac{\rho(q_{e,av})^2}{2g}\right]} = P - P_1 \tag{18}$$

The pressure coefficient for example I is greater along both the inner and outer walls than along the corresponding walls for potential flow, but the difference in pressure coefficients on the two walls at corresponding values of ξ is about the same for both types of flow, indicating that the turning angle of the mean flow is about the same. It is interesting to note that for example I in the vicinity of ξ equals 4.5 the pressure along the outer wall is less than along the inner wall, thus indicating an overturning of the average flow just ahead of this region. The exit pressure coefficient is greater for example I than for the potential flow solution, indicating a smaller pressure drop through the elbow for shear flow. Physically, this smaller pressure drop for example I is explained by the fact that, because of the nonuniform inlet velocity for example I, the average value of H_i (equation (4)) must be greater for example I than for the potential flow solution. But the linear exit velocity distribution for example I is more nearly like that for the potential flow solution (fig. 2); and, therefore, because the average value of H is higher for example I, P_e is also higher.

Numerical Example II

Inlet velocity distribution. - In example II a sinusoidal distribution of velocity across the inlet was prescribed (fig. 8) such that the velocity Q is zero on both walls and the arithmetic average value of Q is 0.5 (same as example I). Thus,

$$Q_i = \frac{\pi}{4} \sin \pi\eta \tag{19a}$$

This sinusoidal variation in velocity approximates the parabolic distribution for fully developed laminar flow in a straight duct with parallel walls. For the inlet velocity distribution given by equation (19a) the distribution of H is (appendix E)

$$H = H_0 + \frac{\pi^2}{4}(\Psi - \Psi^2) \tag{19b}$$

Therefore, the vorticity of the shear flow becomes

$$\zeta = -\frac{1}{2}\frac{dH}{d\Psi} = -\frac{\pi^2}{8} + \frac{\pi^2}{4}\Psi \tag{19c}$$

so that for a sinusoidal inlet velocity distribution the vorticity is a linear function of Ψ. Also, for the sinusoidal inlet velocity distribution given by equation (19a) it can be shown that (appendix E)

$$\Psi_i = \frac{1}{2}(1 - \cos \pi\eta_i) \tag{19d}$$

$$\Psi_e = \frac{1}{2}\left(1 - \cos\frac{\pi}{2}\eta_e + \sin\frac{\pi}{2}\eta_e\right) \tag{19e}$$

and

$$Q_e = \frac{\pi}{4}\left(\sin\frac{\pi}{2}\eta_e + \cos\frac{\pi}{2}\eta_e\right) \tag{19f}$$

The exit velocity distribution is compared with the inlet distribution in figure 8.

Streamlines. - The streamlines of example II are presented in figure 9. An eddy has formed on the outer wall and extends from $\xi \approx -7.25$ to $\xi \approx 2.0$. (In theory this eddy extends upstream to minus infinity but becomes extremely narrow so that within the accuracy of relaxation methods it disappears at $\xi \approx -7.25$.) This eddy occurs because, as in example I, the velocity decelerates along the outer wall. Because the velocity was initially zero at this wall, the flow therefore reverses itself and an eddy is formed. Three stagnation points occur for the eddy: two on the outer wall (one downstream at infinity, theoretically, and the other at ξ approximately equal to 2.0) and a third in the center of the eddy near $\xi \approx -0.375$. The maximum velocities occur near the center of the channel as indicated by the narrow spacing of the streamlines.

Velocity distribution. - Lines of constant resultant velocity Q are presented in figure 10. The velocity component Q_η normal to potential flow streamlines is shown in figure 11. This distribution of Q_η appears similar to that for example I (fig. 5). However, the magnitudes of Q_η are greater in example II and both positive and negative values exist. A minimum point occurs at $\xi \approx 0.375$, $\eta \approx 0.250$ and a maximum at $\xi \approx 2.750$, $\eta \approx 0.625$. As for example I, these points occur for reasons already discussed in connection with equation (17). This velocity component changes sign because the angle $(\theta - \theta_o)$ (see fig. 1) changes sign as indicated in figure 9 where the streamlines for the shear flow are inclined toward the inner wall with respect to the potential streamlines (constant η) in the first half of the elbow and are in inclined toward the outer wall in the second half. A line of zero Q_η occurs along which the streamlines for shear flow are parallel to the streamlines for potential flow.

The velocities along the inner and outer walls are plotted against ξ in figure 12 for example II and for the potential flow solution. For the shear flow solution, the velocities on the inner and outer walls converge to zero upstream at infinity. As for example I, the flow decelerates slightly along the outer wall upstream of the region of turning, but unlike example I, a larger deceleration also occurs along the inner wall in the downstream half of the elbow.

The pressure coefficient $(P - P_i)$ along the inner and outer walls for example II and for the potential flow solution are presented in figure 13. The pressure coefficient for example II converges to zero farther upstream of the region of turning than for potential flow. For reasons already discussed under example I the exit pressure coefficient is greater for example II than for the potential flow solution.

SUPERPOSITION OF SOLUTIONS

The solutions for example I and for potential flow can be combined in linear combinations using the principle of superposition of solutions. In example II the principle of superposition of solutions does not apply, because for this solution the right-hand side of the flow equation (10) is a function of the dependent variable Ψ.

Pure shear flow for example I. - The streamlines for pure shear flow are obtained by subtracting the stream function for potential flow from that for example I. Thus the pure shear flow solution is the solution for which the net mass flow from wall to wall across lines of constant ξ is equal to zero. The stream function for pure shear flow is zero on both walls and negative throughout the channel. Lines of constant percentage of minimum stream function are presented in figure 14. The inlet velocity profile for the pure shear flow is linear varying from -0.25 to 0.25. Velocities are negative along the inner wall and positive along the outer wall. The average velocity across any line of constant ξ is zero and hence the flow is an eddy occupying the entire channel. The streamlines all begin and end at the inlet; the zero streamlines (walls) extend infinitely far downstream. The pure shear flow has no important physical significance and is of interest only mathematically. The solution corresponds to fluid motion in the elbow with zero average flow rate but with the elbow rotating in its plane with a constant angular velocity equal to one-half the vorticity of example I.

Separated flow. - If 25 percent, for example, of the potential flow solution is added to the pure shear flow just discussed, the case of a separated flow on the inner wall upstream of the region of turning is obtained. The streamlines for this flow are presented in figure 15. The separated flow upstream of the region of turning is forced to reattach by the acceleration of the flow through the elbow. The solution can also be reversed, in which case the flow enters at the end with smaller cross section; and the solution in figure 15 shows flow separation resulting from deceleration. Thus, some aspects of boundary-layer behavior can be demonstrated by shear flow solutions that ignore viscous forces in the immediate vicinity of the solution.

Various percentages of pure shear flow. - The potential flow solution was added to various percentages of the pure shear flow solution, resulting in the inlet velocity profiles shown in figure 16. These velocity profiles are for flows with varying amounts of vorticity. The velocities along the inner and outer walls are shown in figures 17(a) and 17(b). The velocities decrease on the inner wall and increase on the outer wall as the negative vorticity increases so that the curves for the inner and outer walls cross. Negative values of Q along the inner wall would indicate the presence of a separated flow region on this wall. The deceleration before turning becomes more pronounced as the negative vorticity increases.

The pressure coefficient $(P - P_1)$ along the channel walls is shown in figure 18. The pressure coefficient along each wall increases as the vorticity increases. As a result, the static pressure drop through the elbow becomes less as the percentage of pure rotational flow becomes larger. The reasons for this behavior have already been discussed under example I.

The difference in pressure coefficient across the channel at any line of constant ξ is nearly the same for all the cases considered in figure 18. This fact is shown in figure 19 where the difference in pressure coefficient $\Delta(P - P_1)$ is plotted against ξ.

SUMMARY OF RESULTS

A method of analysis is developed for two-dimensional shear flows in channels of arbitrary shape. Solutions were obtained for shear flows in a 90° elbow with linear and sinusoidal velocity distributions across the inlet. Several linear combinations of the potential flow solution and the solution for linear inlet velocity distribution were made to obtain: (1) the pure shear flow solution (negative vorticity), (2) a solution that is representative in some respects of the behavior of a separated boundary layer under accelerating flow conditions, and (3) a series of solutions with equal increments of negative vorticity. The solutions indicated that:

1. The drop in static pressure across the accelerating elbow decreased as the vorticity of the shear flow increased. This behavior is explained by the increased nonuniformity of the inlet velocity with increased vorticity.

2. For linear inlet velocity distributions local deceleration along the outer channel wall increased as the negative vorticity of the shear flow increased. However, for the sinusoidal velocity distribution local decelerations occurred on both walls.

3. For linear inlet velocity distributions, as the negative vorticity of the shear flow increased, the magnitude of the velocities increased on the outer wall and decreased on the inner wall, the local pressure coefficients increased gradually, and the difference in local pressure coefficient on the two walls at corresponding points was practically unchanged.

Lewis Flight Propulsion Laboratory
National Advisory Committee for Aeronautics
Cleveland, Ohio, April 16, 1952

APPENDIX A

SYMBOLS

The following symbols are used in this report:

A	area of region in plane of elbow
g	acceleration due to gravity
H	Bernoulli constant, dimensionless, equation (3a)
h	Bernoulli constant, dimensional, equation (3)
N	distance along outer normal to streamline, dimensionless, expressed as ratio of w_e
P	static pressure, dimensionless, equation (1c)
$P-P_1$	local pressure coefficient, equation (18)
$\Delta(P-P_1)$	difference in local pressure coefficient across channel along line of constant ξ
p	static pressure, dimensional
Q	resultant velocity, dimensionless, equation (3b)
q	resultant velocity, dimensional
S	distance along streamline, dimensionless, expressed as ratio of w_e
U	velocity component in X-direction, dimensionless, equation (1d)
u	velocity component in X-direction, dimensional
V	velocity component in Y-direction, dimensionless, equation (1d)
v	velocity component in Y-direction, dimensional
w	width of elbow, dimensional
X,Y	Cartesian coordinates, dimensionless, equation (1d)
x,y	Cartesian coordinates, dimensional

ζ	vorticity, equation (11)
η	stream function for potential flow solution, equation (12a)
θ	angle between X-axis and streamline measured positive in counterclockwise direction
ξ	velocity potential function for potential flow solution, equation (12a)
ρ	fluid weight density
Ψ	stream function for rotational flow, dimensionless, equation (6a)

Subscripts:

0	conditions along $\eta = 0$
av	average condition across the channel
e	conditions at exit, downstream at infinity
i	conditions at inlet, upstream at infinity
min	minimum
o	conditions in potential flow solution
η	component in η-direction
ξ	component in ξ-direction

APPENDIX B

TRANSFORMATION OF DIFFERENTIAL EQUATION OF FLOW FROM XY- TO $\xi\eta$-PLANE

By definition ξ and η satisfy the Cauchy-Riemann differential equations, equations (12a), so that

$$\left.\begin{aligned} \frac{\partial^2 \xi}{\partial X^2} + \frac{\partial^2 \xi}{\partial Y^2} &= 0 \\ \frac{\partial^2 \eta}{\partial X^2} + \frac{\partial^2 \eta}{\partial Y^2} &= 0 \end{aligned}\right\} \tag{B1}$$

In order to transform the coordinates of equation (10), the following relations were used

$$\frac{\partial^2 \Psi}{\partial X^2} = \frac{\partial^2 \Psi}{\partial \xi^2}\left(\frac{\partial \xi}{\partial X}\right)^2 + 2\frac{\partial^2 \Psi}{\partial \xi \partial \eta}\frac{\partial \xi}{\partial X}\frac{\partial \eta}{\partial X} + \frac{\partial^2 \Psi}{\partial \eta^2}\left(\frac{\partial \eta}{\partial X}\right)^2 + \frac{\partial \Psi}{\partial \xi}\frac{\partial^2 \xi}{\partial X^2} + \frac{\partial \Psi}{\partial \eta}\frac{\partial^2 \eta}{\partial X^2}$$

$$= U_o^2 \frac{\partial^2 \Psi}{\partial \xi^2} - 2U_oV_o\frac{\partial^2 \Psi}{\partial \xi \partial \eta} + V_o^2\frac{\partial^2 \Psi}{\partial \eta^2} + \frac{\partial \Psi}{\partial \xi}\frac{\partial^2 \xi}{\partial X^2} + \frac{\partial \Psi}{\partial \eta}\frac{\partial^2 \eta}{\partial X^2} \tag{B2a}$$

$$\frac{\partial^2 \Psi}{\partial Y^2} = \frac{\partial^2 \Psi}{\partial \xi^2}\left(\frac{\partial \xi}{\partial Y}\right)^2 + 2\frac{\partial^2 \Psi}{\partial \xi \partial \eta}\frac{\partial \xi}{\partial Y}\frac{\partial \eta}{\partial Y} + \frac{\partial^2 \Psi}{\partial \eta^2}\left(\frac{\partial \eta}{\partial Y}\right)^2 + \frac{\partial^2 \xi}{\partial Y^2}\frac{\partial \Psi}{\partial \xi} + \frac{\partial^2 \eta}{\partial Y^2}\frac{\partial \Psi}{\partial \eta}$$

$$= V_o^2 \frac{\partial^2 \Psi}{\partial \xi^2} + 2U_oV_o\frac{\partial^2 \Psi}{\partial \xi \partial \eta} + U_o^2\frac{\partial^2 \Psi}{\partial \eta^2} + \frac{\partial \Psi}{\partial \xi}\frac{\partial^2 \xi}{\partial Y^2} + \frac{\partial \Psi}{\partial \eta}\frac{\partial^2 \eta}{\partial Y^2} \tag{B2b}$$

From equations (10), (B1), (B2a), and (B2b)

$$\frac{\partial^2 \Psi}{\partial \xi^2} + \frac{\partial^2 \Psi}{\partial \eta^2} = \frac{1}{2Q_o^2}\frac{dH}{d\Psi} \tag{13}$$

where

$$Q_o^2 = U_o^2 + V_o^2$$

Equation (13) is the differential equation of flow in ξ,η-coordinates.

APPENDIX C

DERIVATION OF EQUATIONS FOR RESULTANT VELOCITY Q AND ITS COMPONENTS Q_ξ, Q_η, U, AND V

The derivatives of Ψ with respect to ξ and η expressed in terms of X and Y are given by

$$\left.\begin{aligned} \frac{\partial \Psi}{\partial \xi} &= \frac{\partial \Psi}{\partial X}\frac{\partial X}{\partial \xi} + \frac{\partial \Psi}{\partial Y}\frac{\partial Y}{\partial \xi} \\ \text{and} \\ \frac{\partial \Psi}{\partial \eta} &= \frac{\partial \Psi}{\partial X}\frac{\partial X}{\partial \eta} + \frac{\partial \Psi}{\partial Y}\frac{\partial Y}{\partial \eta} \end{aligned}\right\} \tag{C1}$$

But, it can be shown that

$$\left.\begin{aligned} \frac{\partial X}{\partial \xi} &= \frac{\cos \theta_o}{Q_o} \\ \frac{\partial Y}{\partial \xi} &= \frac{\sin \theta_o}{Q_o} \\ \frac{\partial X}{\partial \eta} &= \frac{-\sin \theta_o}{Q_o} \\ \frac{\partial Y}{\partial \eta} &= \frac{\cos \theta_o}{Q_o} \end{aligned}\right\} \tag{C2}$$

so that from equations (6a), (C1), and (C2)

$$\left.\begin{aligned} \frac{\partial \Psi}{\partial \xi} &= -V\frac{\cos \theta_o}{Q_o} + U\frac{\sin \theta_o}{Q_o} \\ \frac{\partial \Psi}{\partial \eta} &= V\frac{\sin \theta_o}{Q_o} + U\frac{\cos \theta_o}{Q_o} \end{aligned}\right\} \tag{C3}$$

From figure 1 it is seen that

$$\left.\begin{aligned} Q_\xi &= Q\cos(\theta-\theta_o) \\ &= Q(\cos\theta\cos\theta_o + \sin\theta\sin\theta_o) \\ &= U\cos\theta_o + V\sin\theta_o \\ Q_\eta &= Q\sin(\theta-\theta_o) \\ &= Q(\sin\theta\cos\theta_o - \sin\theta_o\cos\theta) \\ &= V\cos\theta_o - U\sin\theta_o \end{aligned}\right\} \quad (C4)$$

Finally, from equations (C3) and (C4)

$$Q_\xi = Q_o\frac{\partial\Psi}{\partial\eta} \quad (14b)$$

$$Q_\eta = -Q_o\frac{\partial\Psi}{\partial\xi} \quad (14c)$$

Likewise, from equation (C4)

$$\left.\begin{aligned} U &= Q_\xi\cos\theta_o - Q_\eta\sin\theta_o \\ V &= Q_\xi\sin\theta_o + Q_\eta\cos\theta_o \end{aligned}\right\} \quad (15)$$

APPENDIX D

INLET AND EXIT CONDITIONS FOR EXAMPLE I

At the inlet of the elbow, upstream at infinity, Q_0 is 1/2, Q_η is 0, Q_ξ is equal to Q_i, and Ψ is a function of η only, so that from equations (14b) and (16a)

$$\int_0^{\Psi_i} d\Psi_i = 2\int_0^{\eta_i} (0.25 + 0.50\ \eta_i)\ d\eta_i$$

$$\Psi_i = 0.5(\eta_i + \eta_i^2) \tag{16d}$$

Also, at the inlet P is constant and H and Q are functions of η only, so that from equation (4)

$$2Q_i \left(\frac{dQ}{d\eta}\right)_i = \left(\frac{dH}{d\eta}\right)_i$$

and, therefore, from equation (16a)

$$\int_{H_{i,0}}^{H_i} dH_i = 2\int_0^{\eta_i} (0.25 + 0.50\ \eta_i)\ 0.5\ d\eta_i$$

$$H_i = H_{i,0} + 0.25(\eta_i + \eta_i^2)$$

or from equation (16d) and the fact that H is a function of Ψ only

$$H = H_0 + \frac{\Psi}{2} \tag{16b}$$

At the exit of the elbow, downstream at infinity, Q_0 is 1.0, Q_η is 0, Q_ξ is equal to Q_e, and Ψ is a function of η only. Therefore, from equation (13)

$$\left(\frac{d^2\Psi}{d\eta^2}\right)_e = \frac{1}{4}$$

which, after integration, becomes

$$\Psi_e = 0.875\ \eta_e + 0.125\ \eta_e^2 \qquad (16e)$$

Therefore, from equations (14b) and (16e)

$$Q_e \doteq 0.875 + 0.25\ \eta_e \qquad (16f)$$

APPENDIX E

INLET AND EXIT CONDITIONS FOR EXAMPLE II

At the inlet of the elbow, upstream at infinity, Q_0 is 1/2, Q_η is 0, Q_ξ is equal to Q_i, and Ψ is a function of η only, so that from equations (14b) and (19a)

$$\int_0^{\Psi_i} d\Psi_i = \frac{\pi}{2}\int_0^{\eta_i} \sin \pi\eta_i \, d\eta_i$$

$$\Psi_i = \frac{1}{2}(1-\cos \pi\eta_i) \tag{19d}$$

Also, at the inlet P is constant and H and Q are functions of η only, so that from equation (4)

$$2Q_i \left(\frac{dQ}{d\eta}\right)_i = \left(\frac{dH}{d\eta}\right)_i$$

and, therefore, from equation (19a)

$$\int_{H_{i,0}}^{H_i} dH_i = \frac{\pi^3}{8}\int_0^{\eta_i} \sin \pi\eta_i \cos \pi\eta_i \, d\eta_i$$

$$H_i = H_{i,0} + \left(\frac{\pi}{4}\right)^2 \sin^2 \pi\eta_i$$

or from equation (19d) and the fact that H is a function of Ψ only

$$H = H_0 + \frac{\pi^2}{4}(\Psi - \Psi^2) \tag{19b}$$

At the exit of the elbow, downstream at infinity, Q_0 is 1.0, Q_η is 0, Q_ξ is equal to Q_e, and Ψ is a function of η only. Therefore, from equation (13)

$$\left(\frac{d^2\Psi}{d\eta^2}\right)_e = \frac{\pi^2}{8} - \frac{\pi^2}{4}\Psi$$

which, after integration between limits, becomes

$$W_e = \frac{1}{2}\left(1 - \cos\frac{\pi}{2}\eta_e + \sin\frac{\pi}{2}\eta_e\right) \tag{19e}$$

Therefore, from equations (14b) and (19e)

$$Q_e = \frac{\pi}{4}\left(\sin\frac{\pi}{2}\eta_e + \cos\frac{\pi}{2}\eta_e\right) \tag{19f}$$

REFERENCES

1. Squire, H. B., and Winter, K. G.: The Secondary Flow in a Cascade of Airfoils in a Nonuniform Stream. Jour. Aero. Sci., vol. 18, no. 4. April 1951, pp. 271-277.

2. Hawthorne, William R.: Secondary Circulation in Fluid Flow. Gas Turbine Lab. M.I.T., May 1950.

3. Kronauer, Richard E.: Secondary Flows in Fluid Dynamics. Pratt and Whitney Res. Rep. No. 132, Gordon McKay Lab., Harvard Univ., April 1951.

4. Emmons, Howard W.: The Numerical Solution of Compressible Fluid Flow Problems. NACA TN 932, 1944.

5. Green, J. R., and Southwell, R. V.: Relaxation Methods Applied to Engineering Problems. IX. High-Speed Flow of Compressible Fluid Through a Two-Dimensional Nozzle. Phil. Trans. Roy. Soc. (London), ser. A, vol. 239, 1946, pp. 367-386.

6. Tsien, Hsue-Shen: Symmetrical Joukousky Airfoils in Shear Flow. Quart. Appl. Math., vol. 1, no. 2, July 1943, pp. 130-148.

7. James, D. G.: Two-Dimensional Airfoils in Shear Flow. I. Quart. Jour. Mech. and Appl. Math., vol. IV, pt. 4, Dec. 1951, pp. 407-418.

8. Stanitz, John D.: Design of Two-Dimensional Channels with Prescribed Velocity Distributions Along the Channel Walls. I - Relaxation Solutions. NACA TN 2593, 1952.

9. Southwell, R. V.: Relaxation Methods in Theoretical Physics. Clarendon Press (Oxford), 1946.

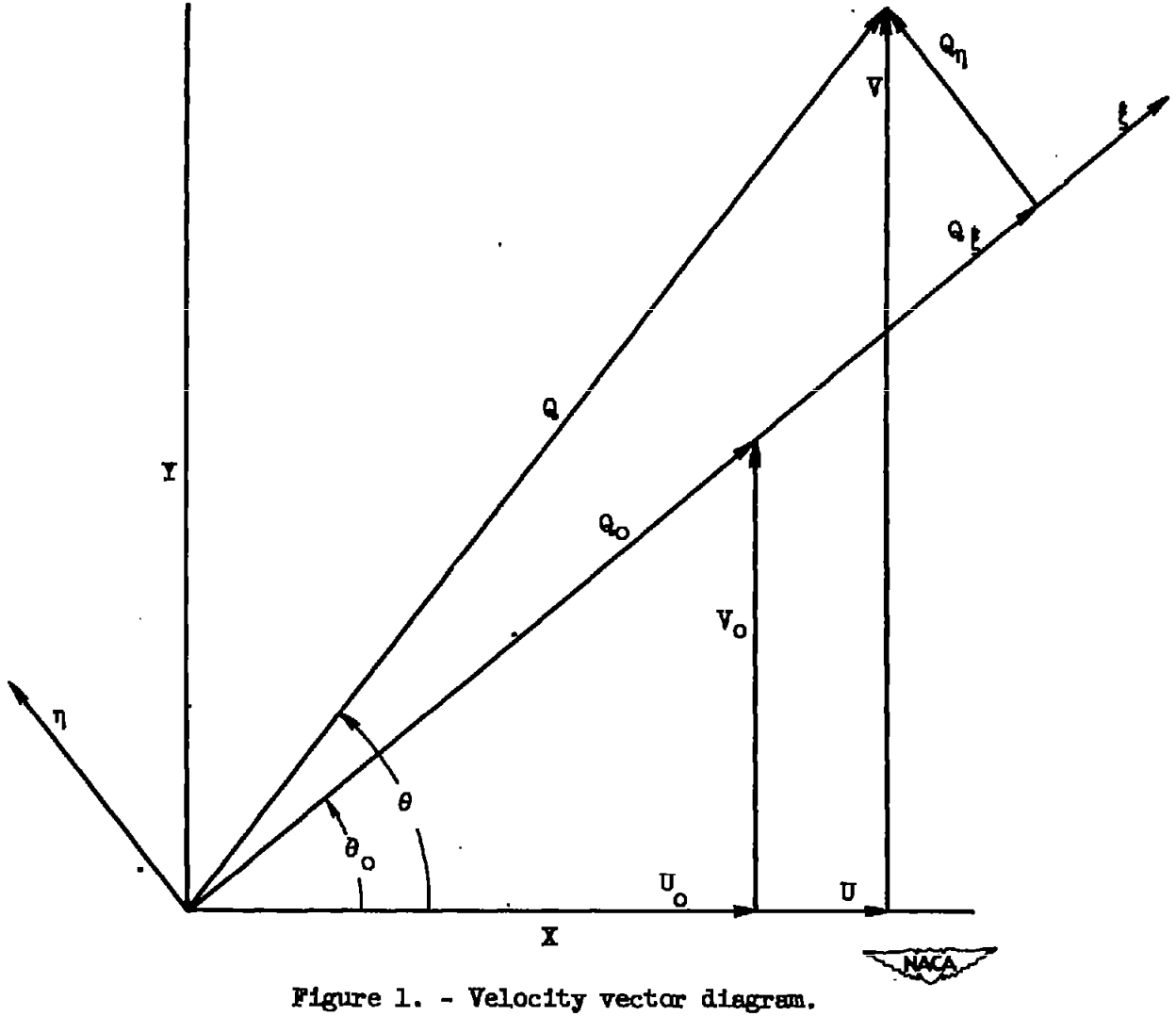

Figure 1. - Velocity vector diagram.

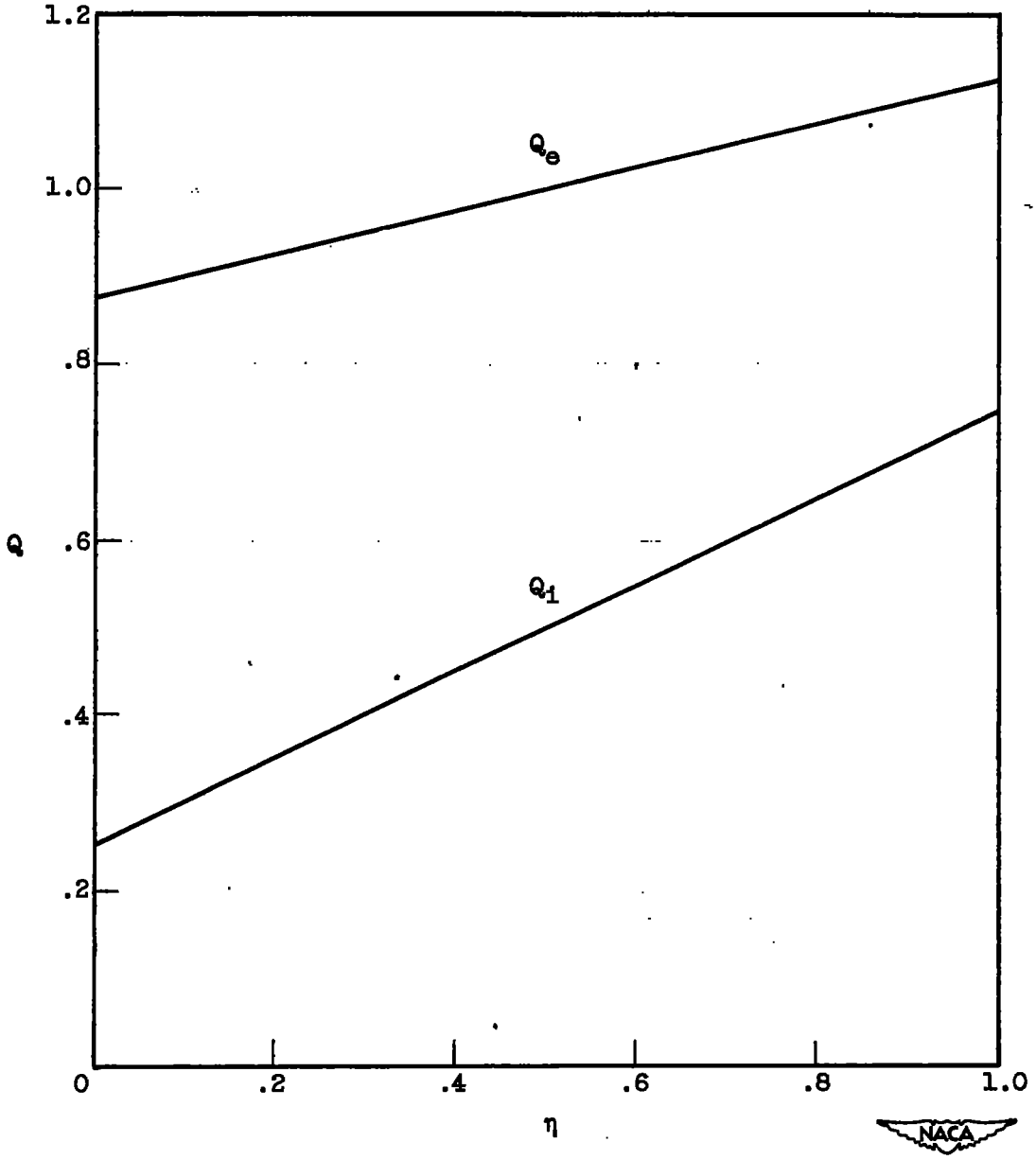

Figure 2. - Inlet and exit velocity profiles for example I.

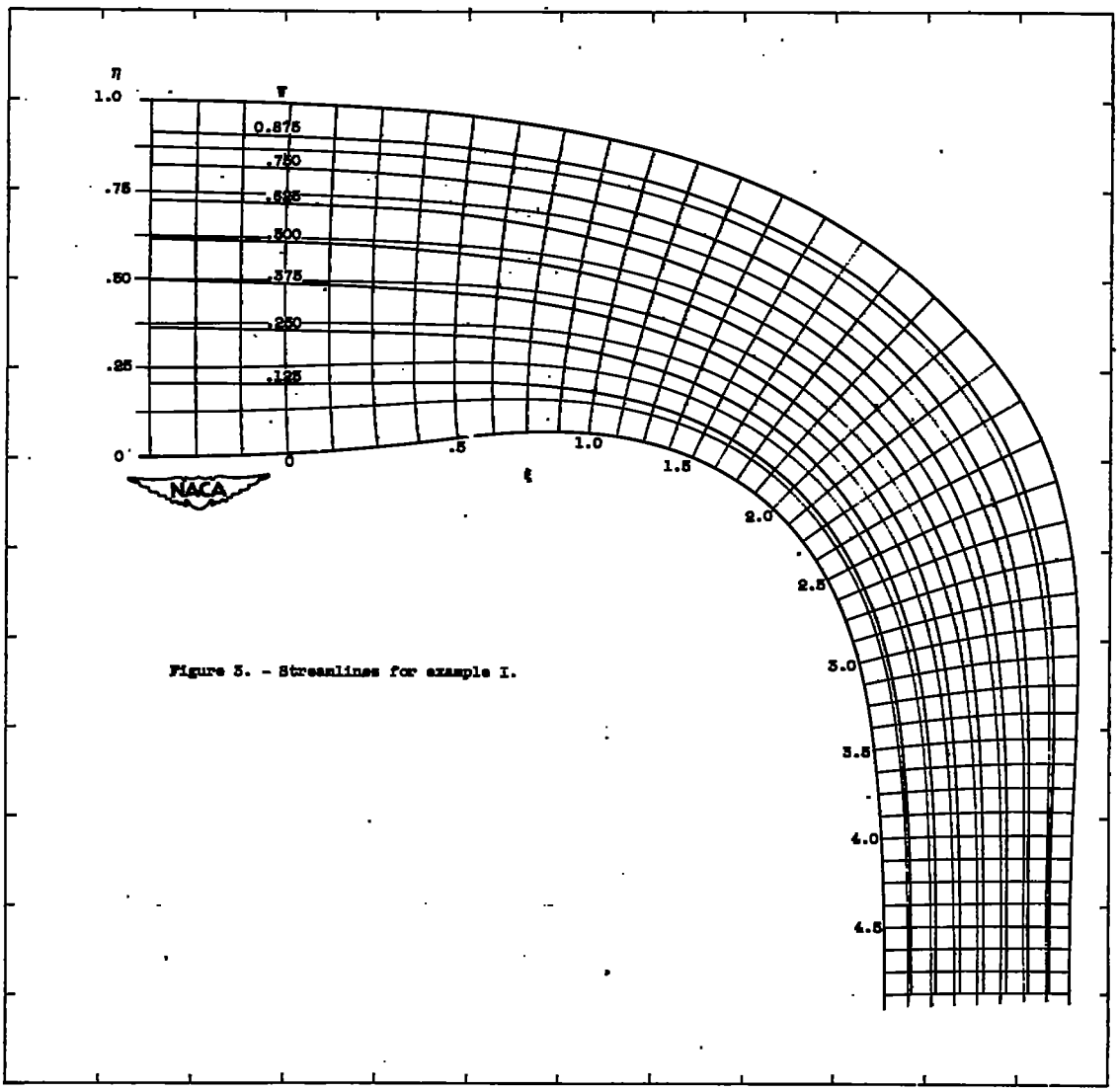

Figure 5. - Streamlines for example I.

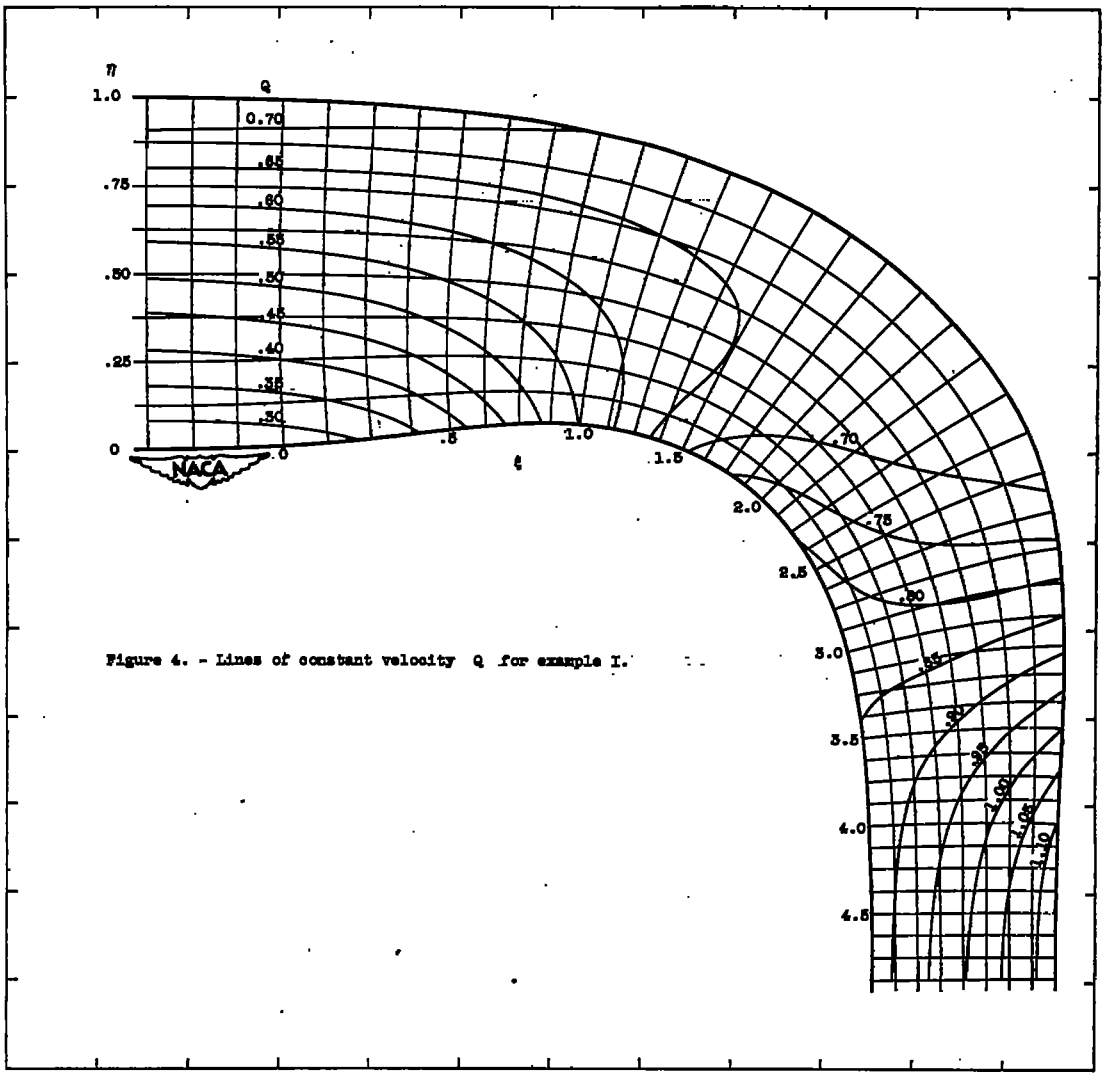

Figure 4. - Lines of constant velocity Q for example I.

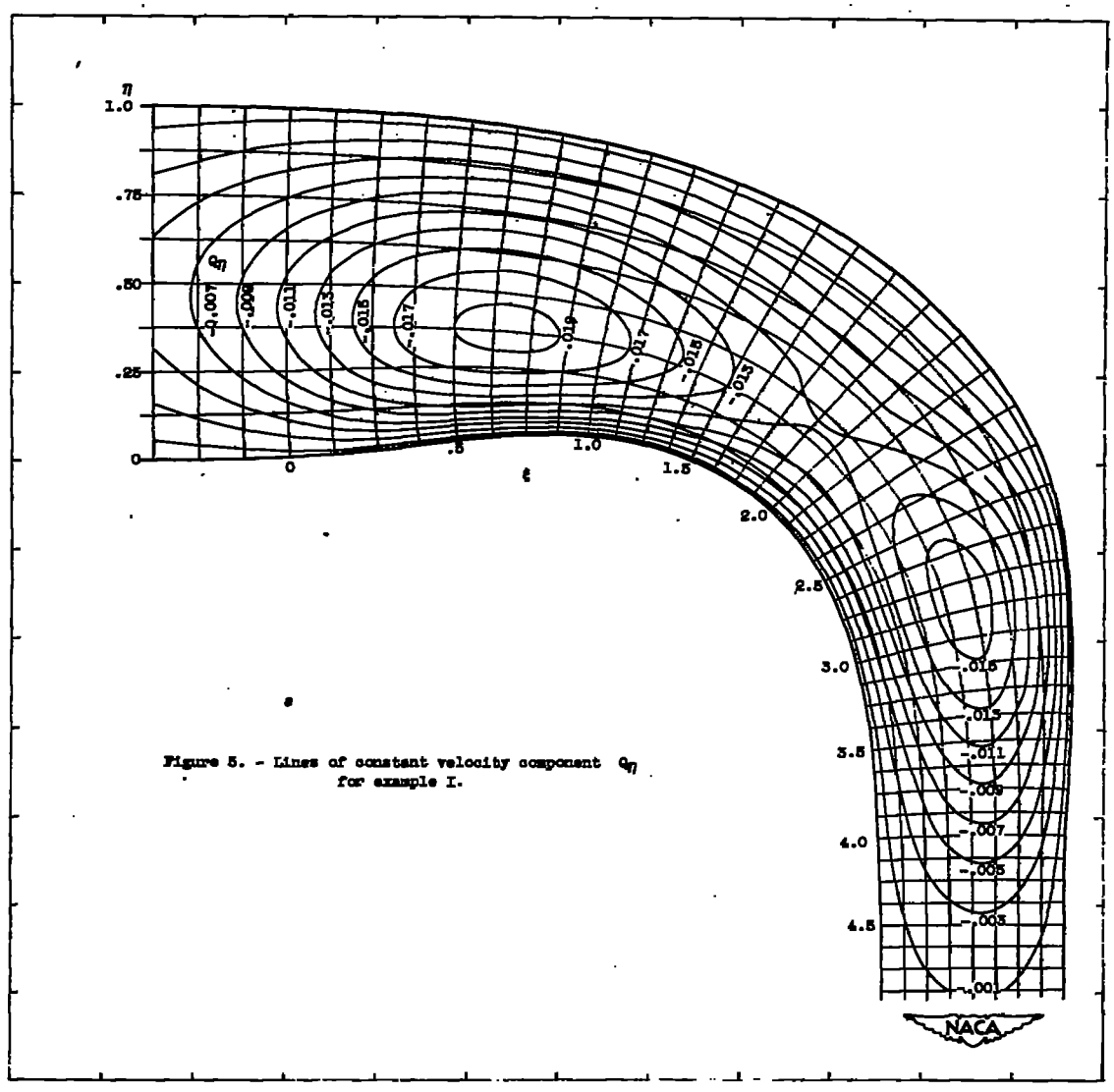

Figure 5. - Lines of constant velocity component Q_η for example I.

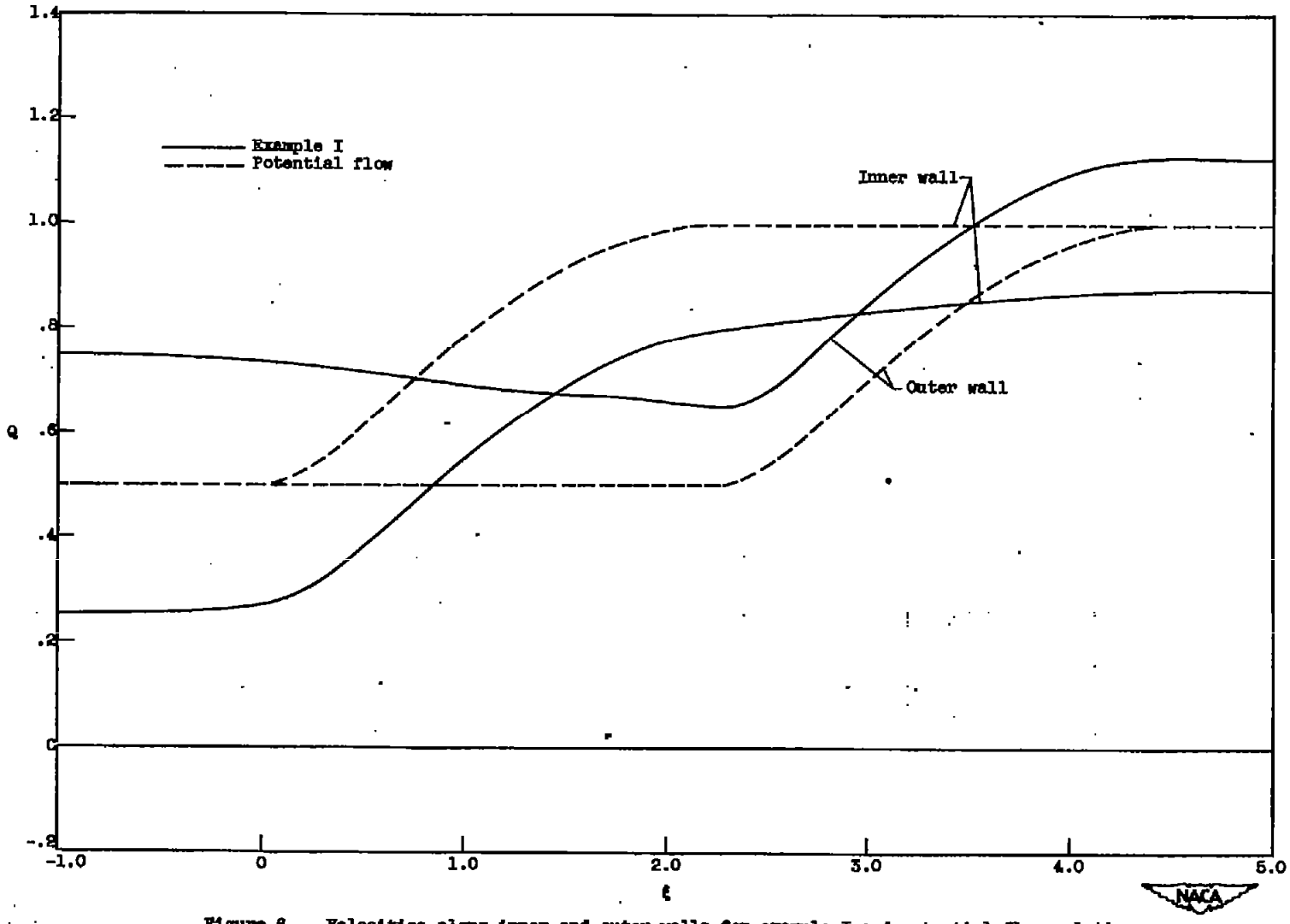

Figure 8. - Velocities along inner and outer walls for example I and potential flow solution.

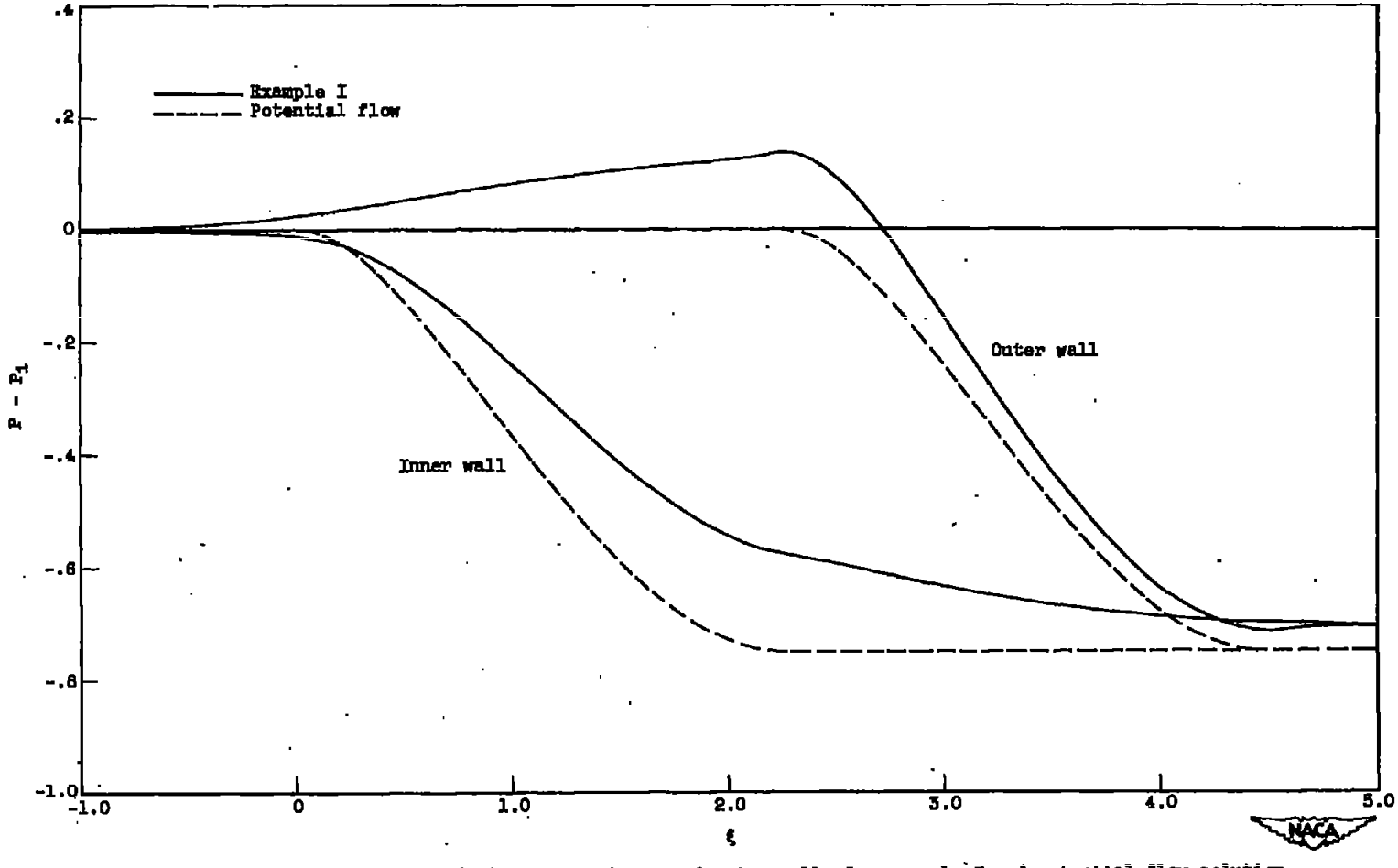

Figure 7. - Pressure coefficient along inner and outer walls for example I and potential flow solution.

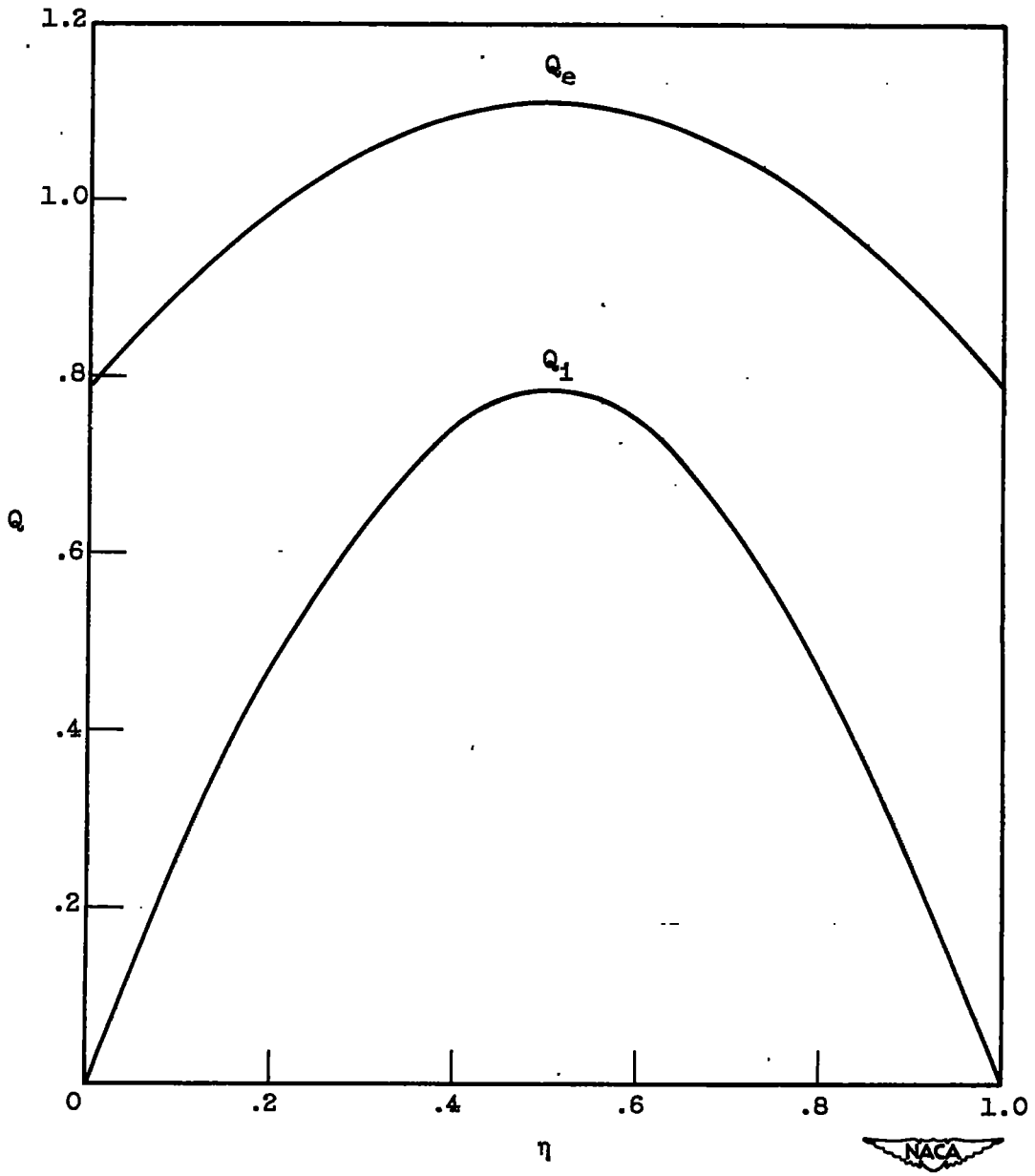

Figure 8. - Inlet and exit velocity profiles for example II.

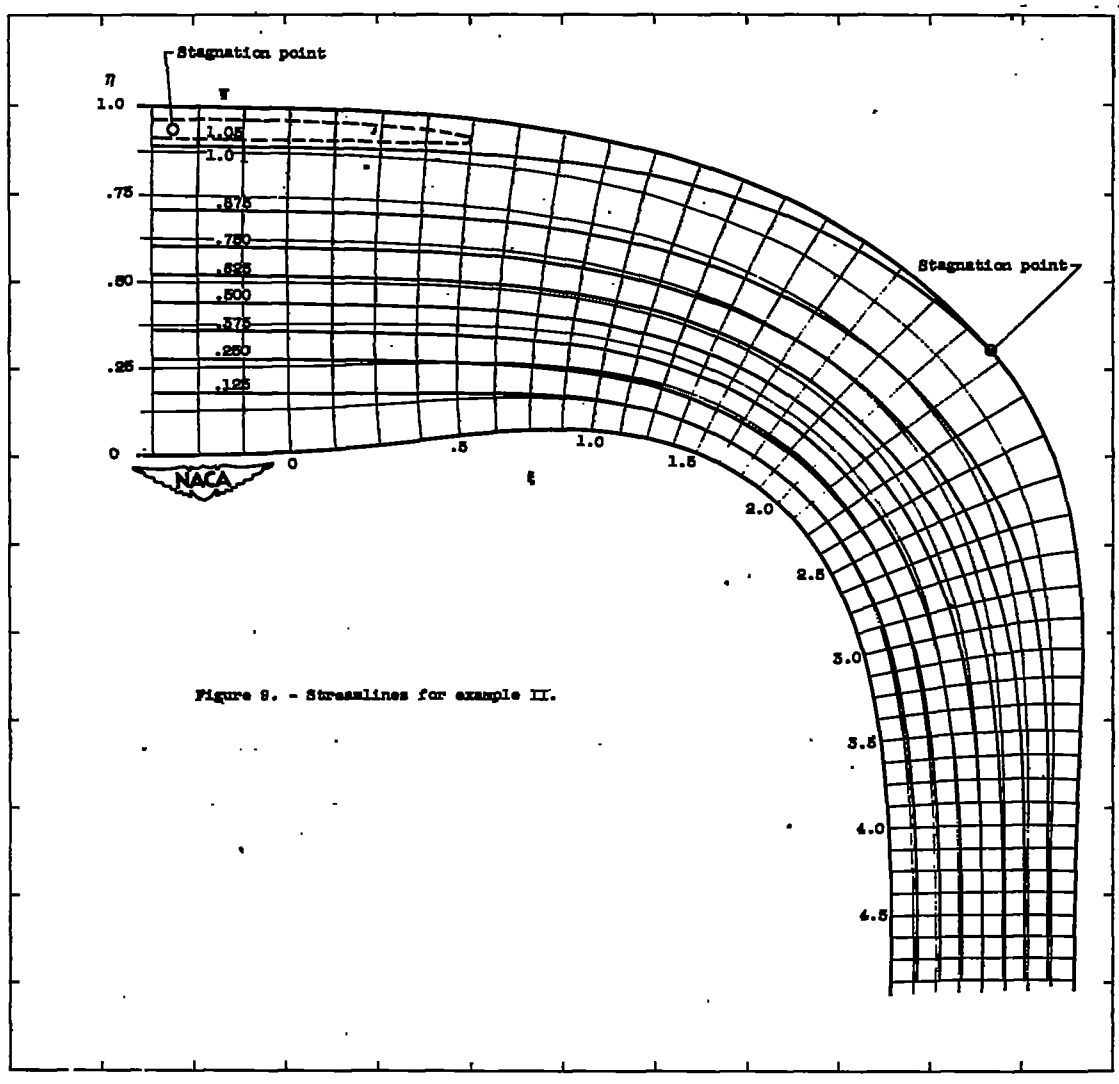

Figure 9. - Streamlines for example II.

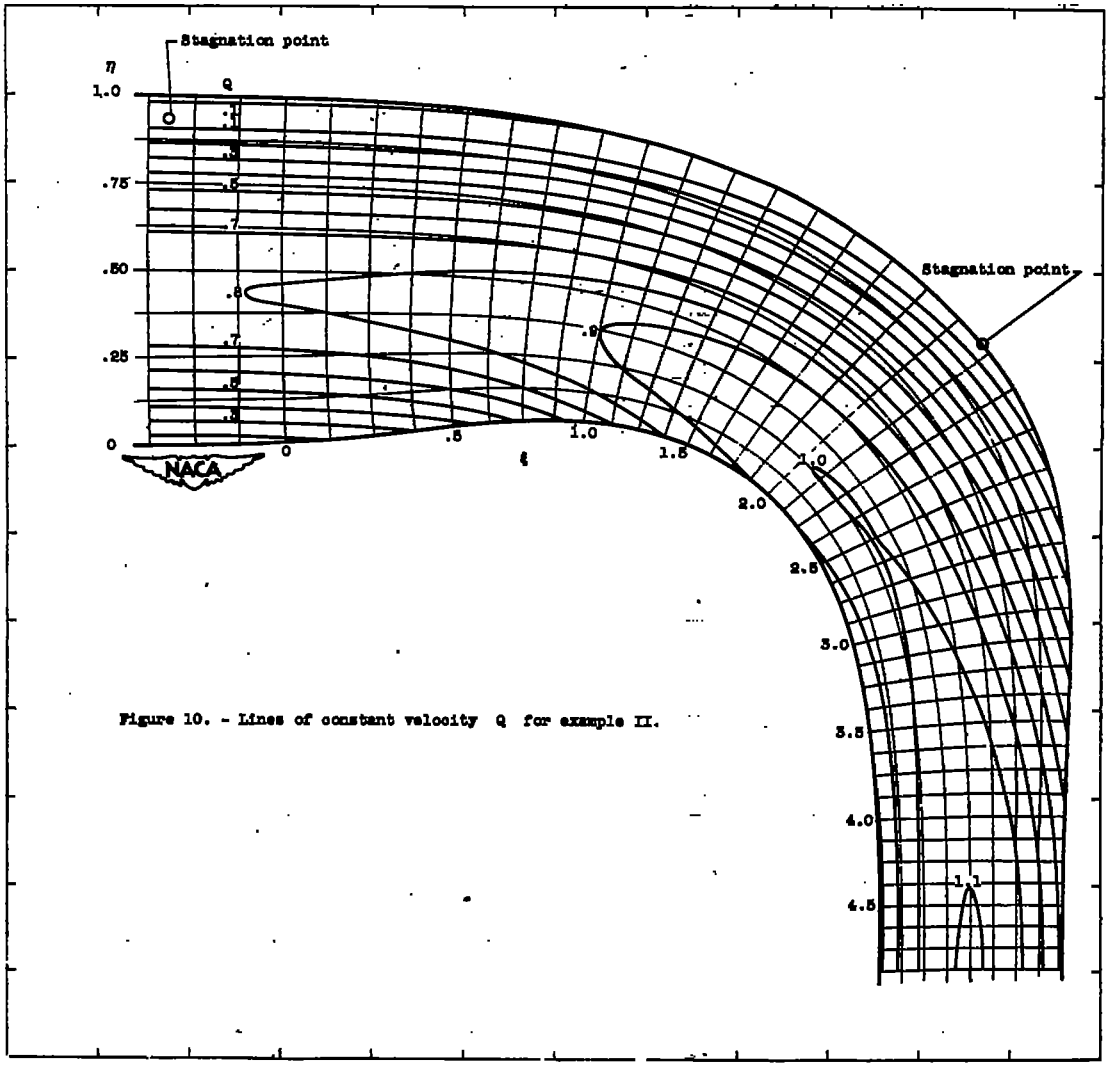

Figure 10. - Lines of constant velocity Q for example II.

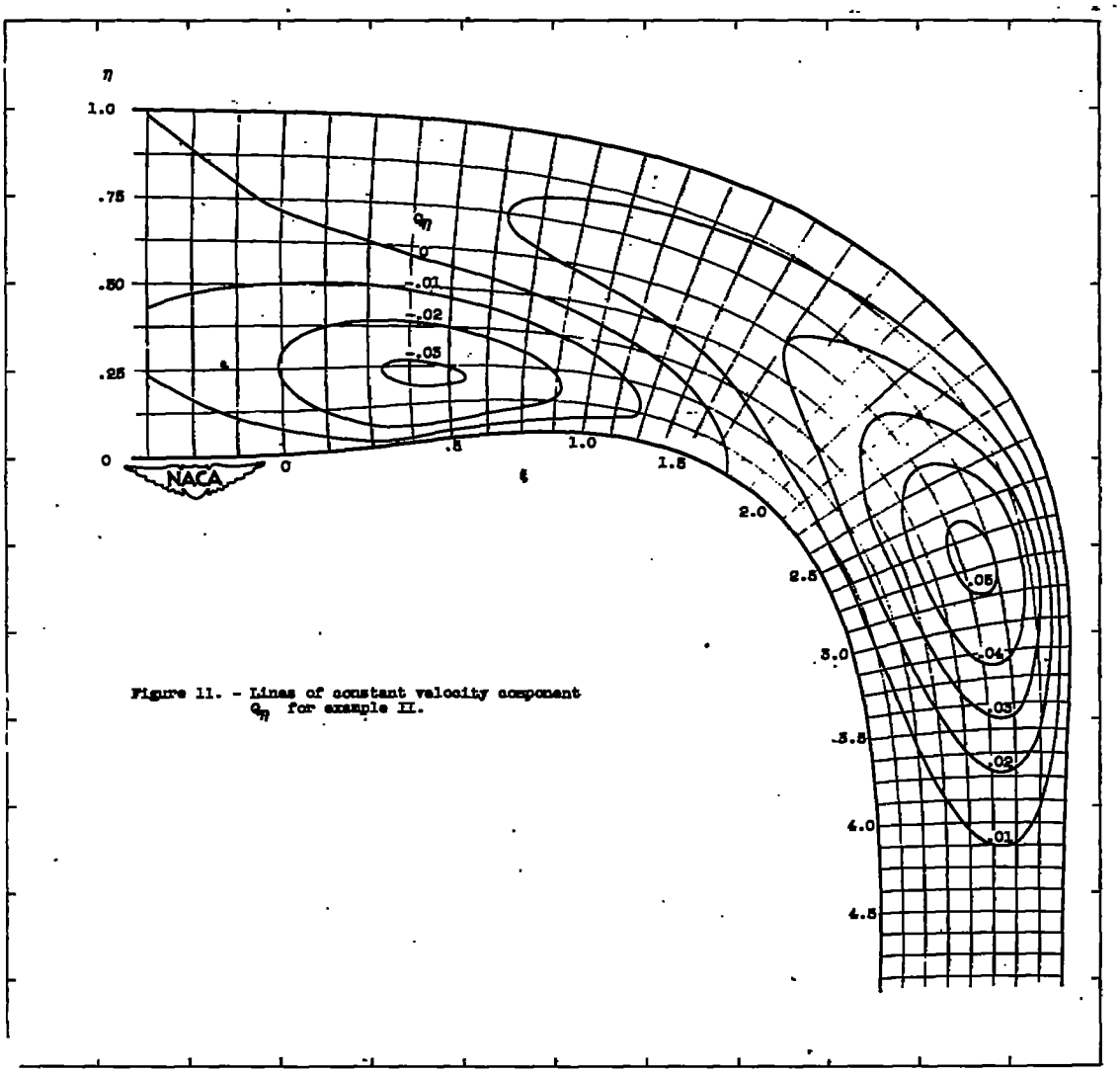

Figure 11. - Lines of constant velocity component q_η for example II.

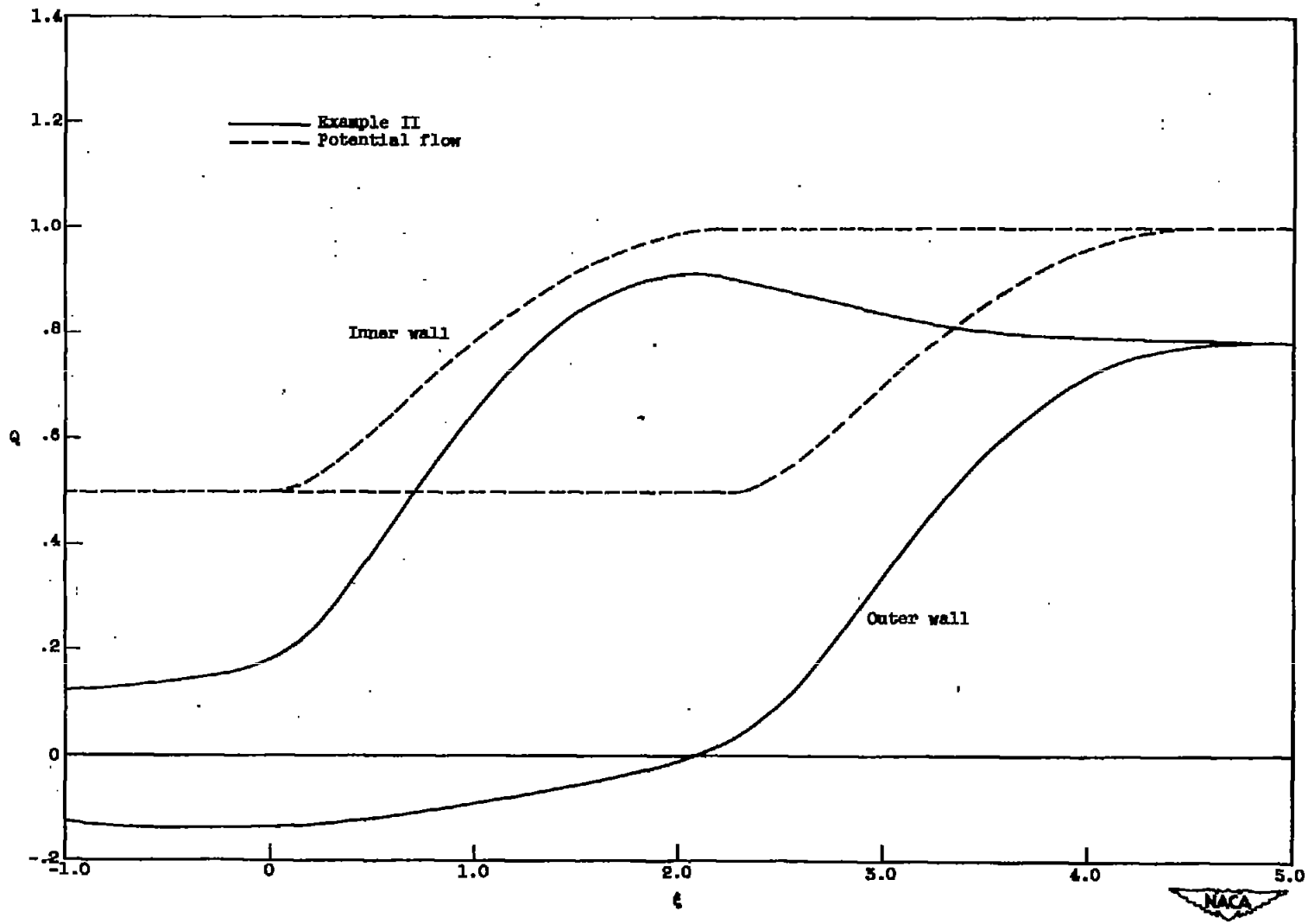

Figure 12. - Velocities along inner and outer walls for example II and potential flow solution.

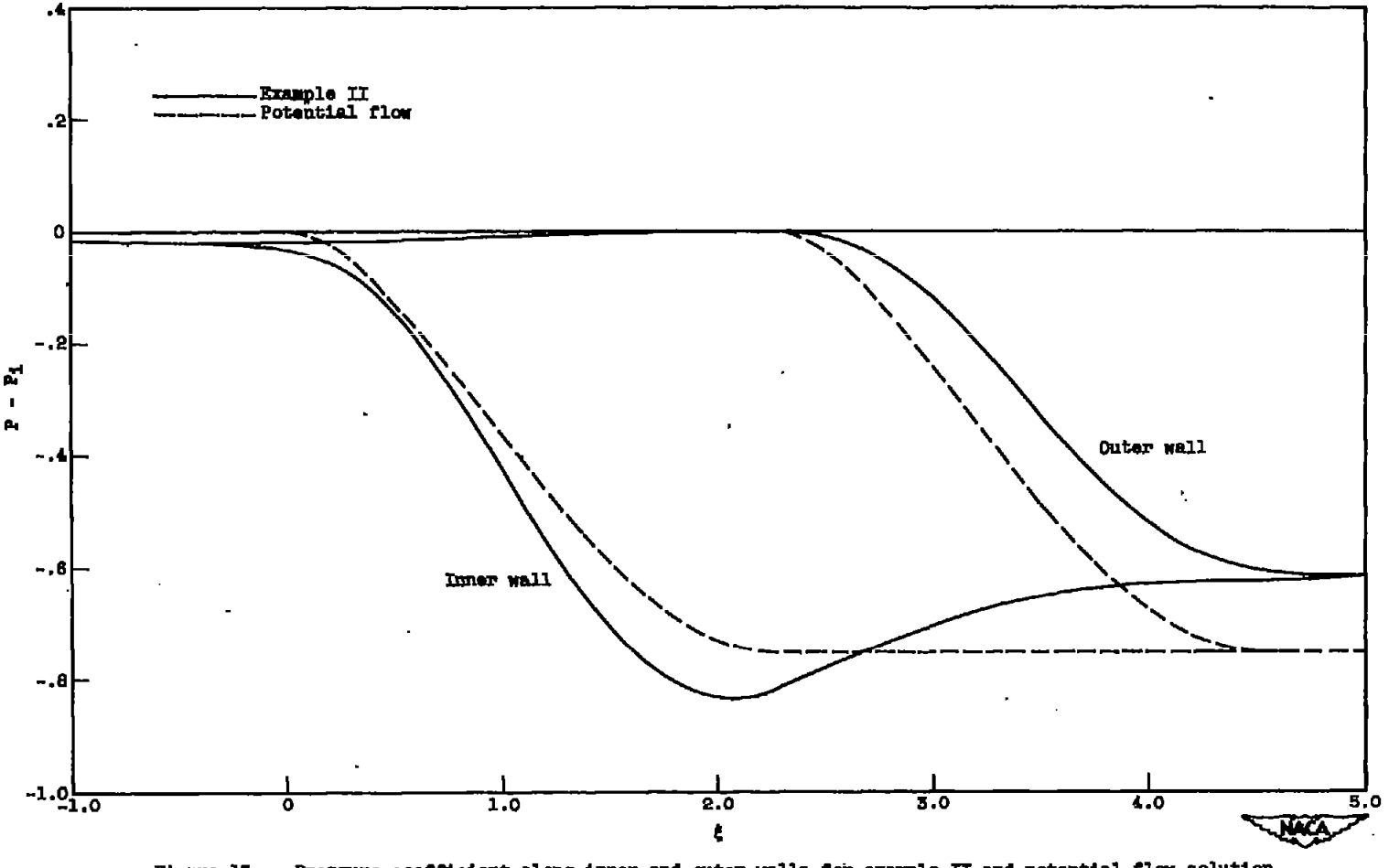

Figure 13. - Pressure coefficient along inner and outer walls for example II and potential flow solution.

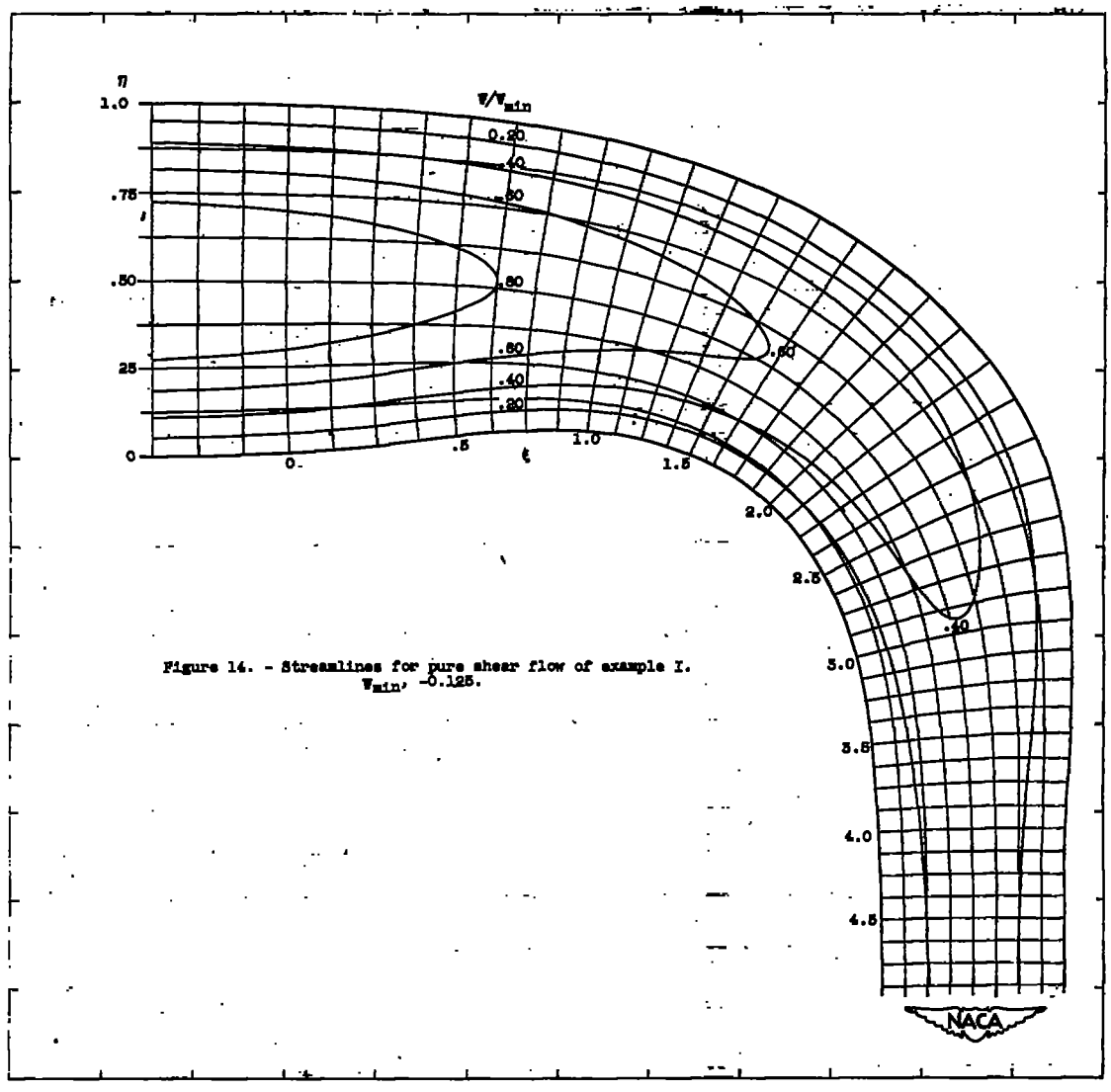

Figure 14. - Streamlines for pure shear flow of example I. ψ_{min}, -0.125.

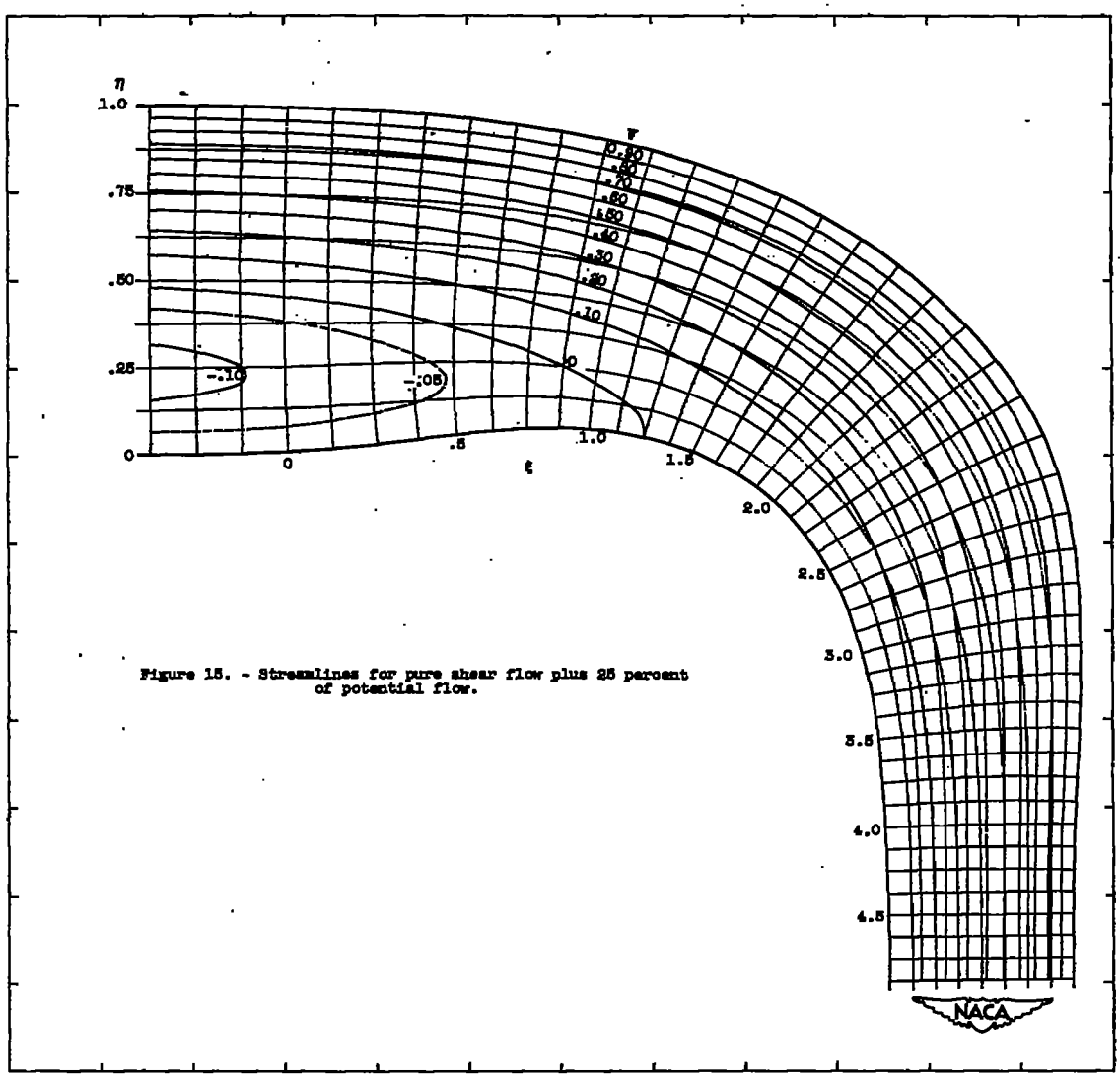

Figure 15. - Streamlines for pure shear flow plus 25 percent of potential flow.

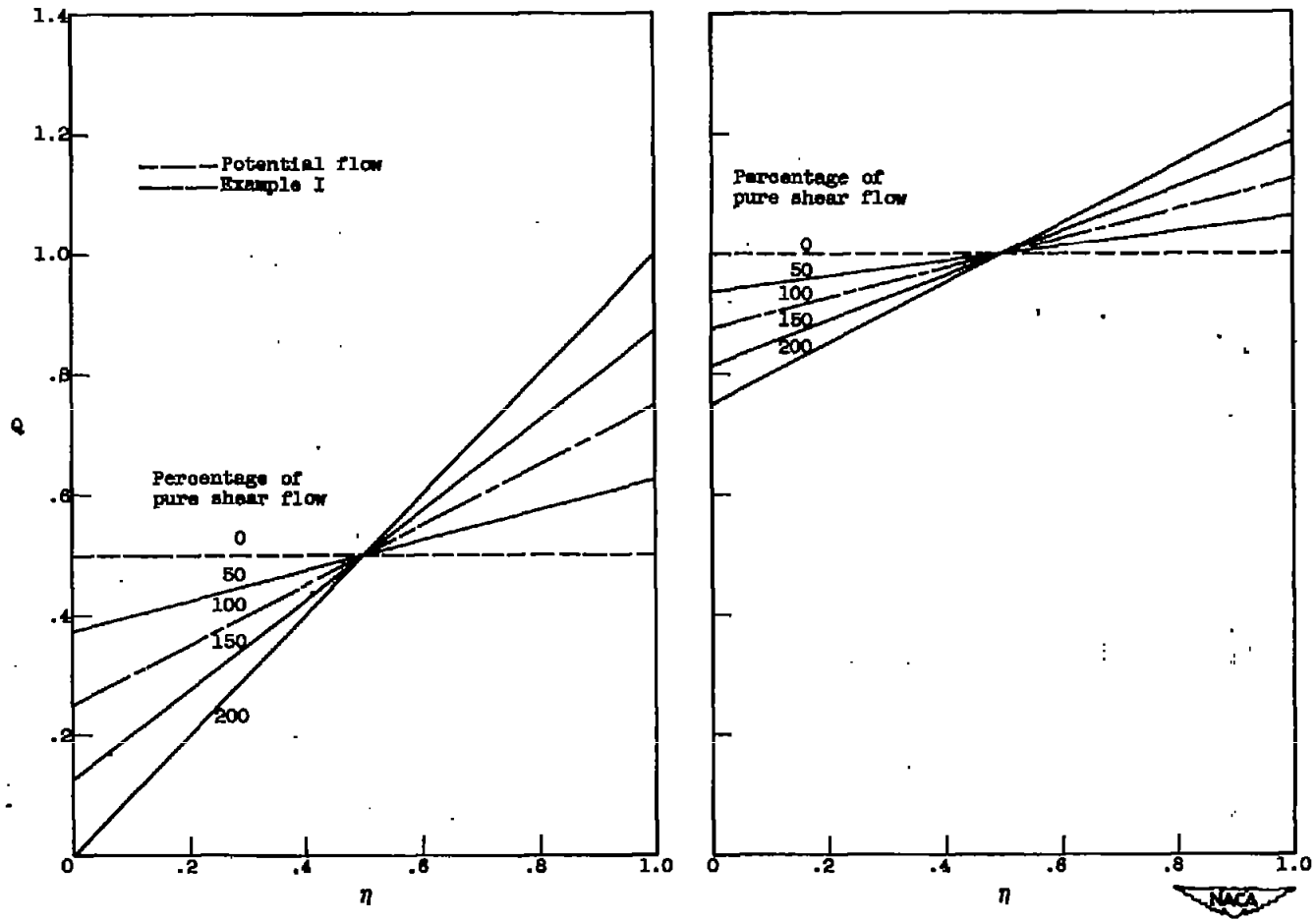

(a) Elbow inlet, upstream at infinity.

(b) Elbow exit, downstream at infinity.

Figure 16. - Inlet and exit velocity profiles for potential flow plus various percentages of pure shear flow.

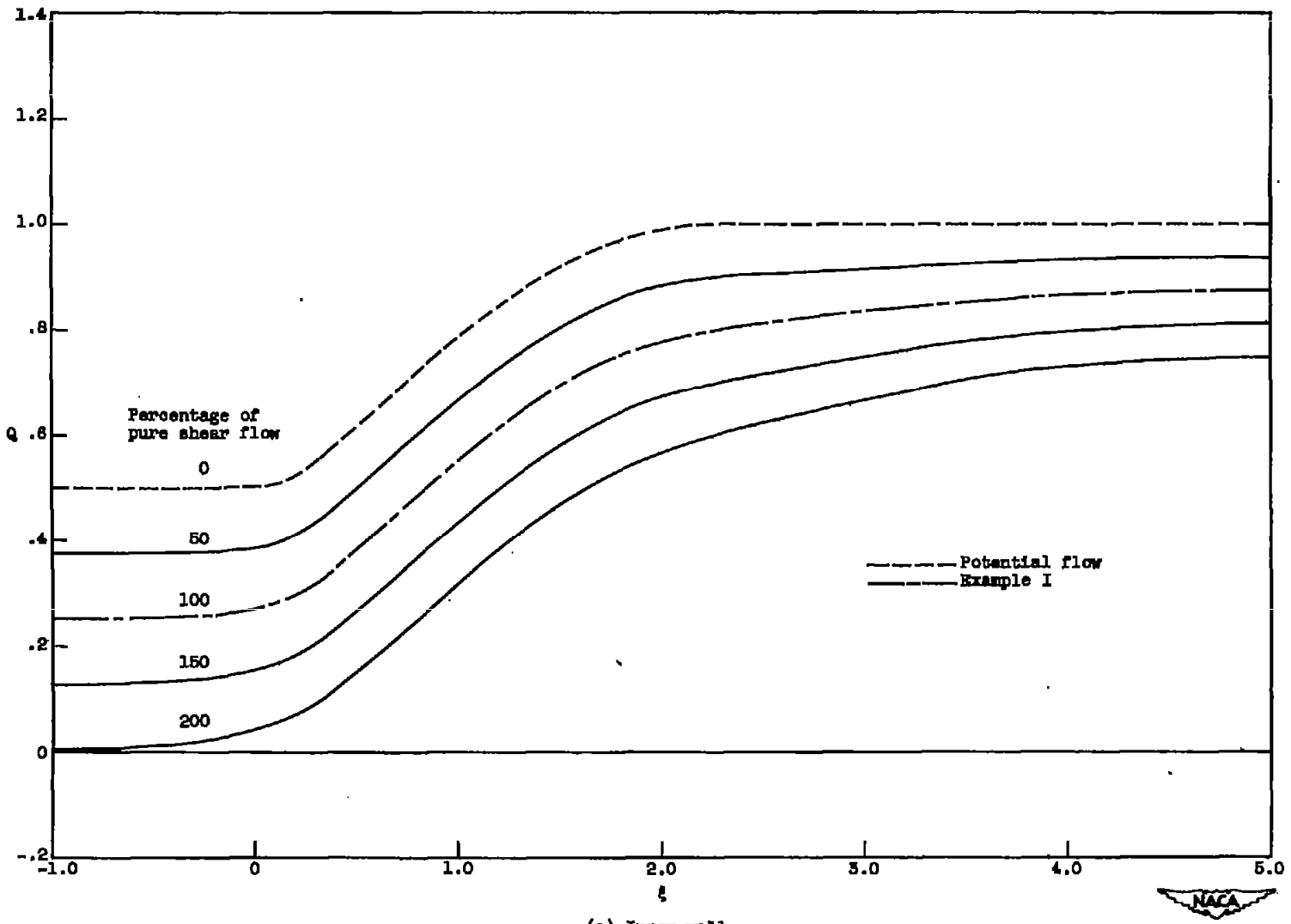

(a) Inner wall.

Figure 17. - Velocities along inner and outer walls for potential flow plus various percentages of pure shear flow.

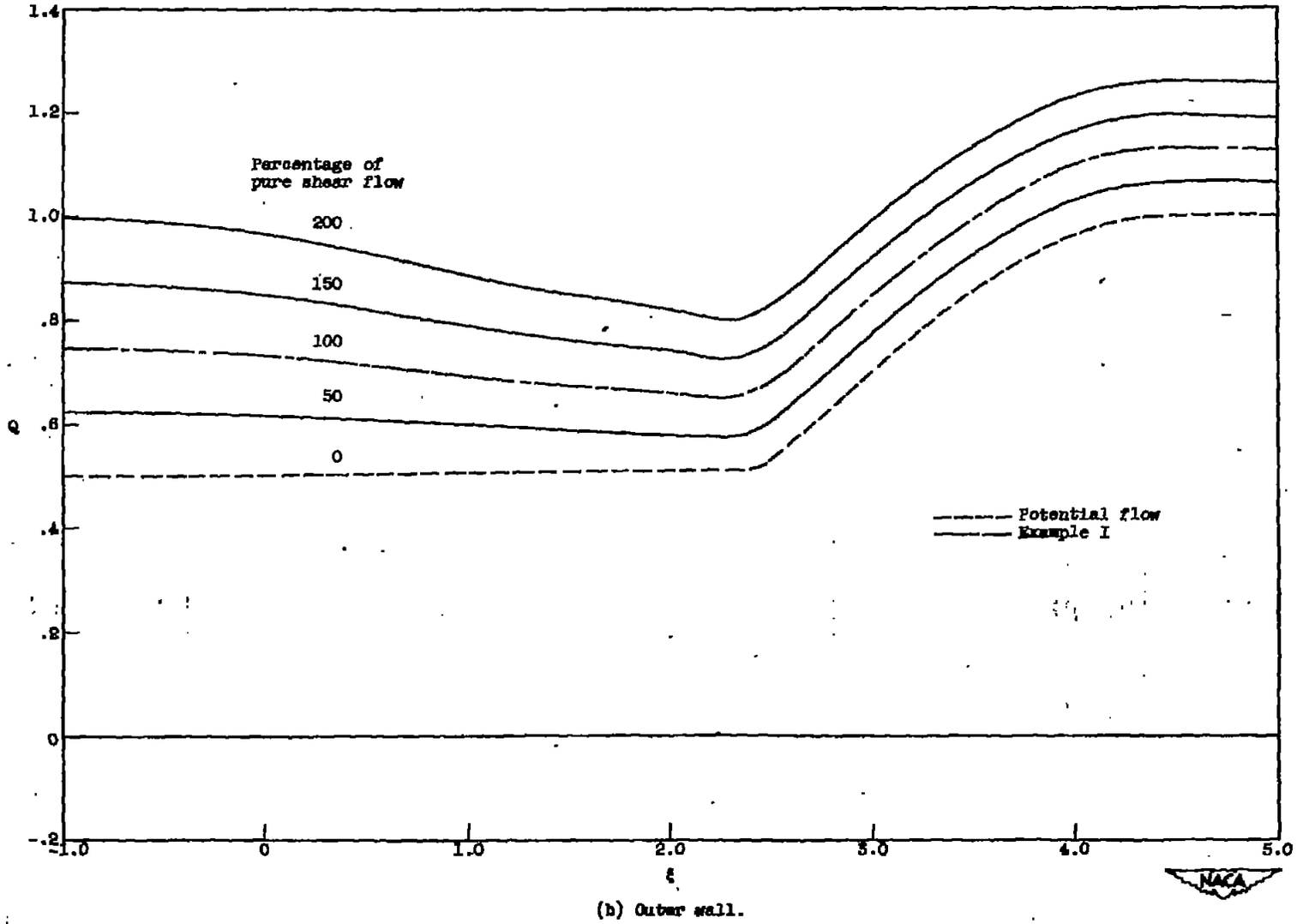

(b) Outer wall.

Figure 17. - Concluded. Velocities along inner and outer walls for potential flow plus various percentages of pure shear flow.

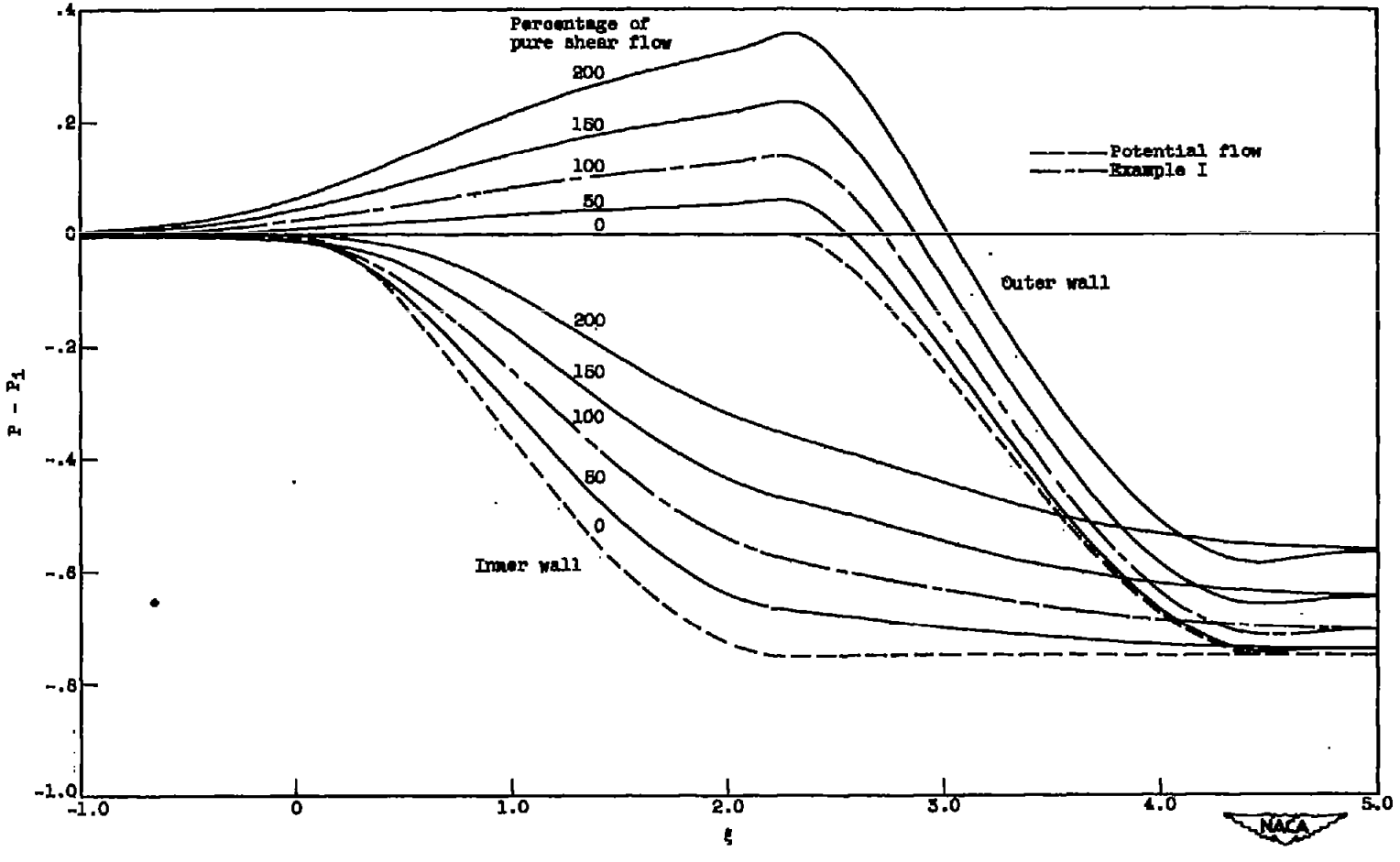

Figure 18. - Pressure coefficient along inner and outer walls for potential flow plus various percentages of pure shear flow.

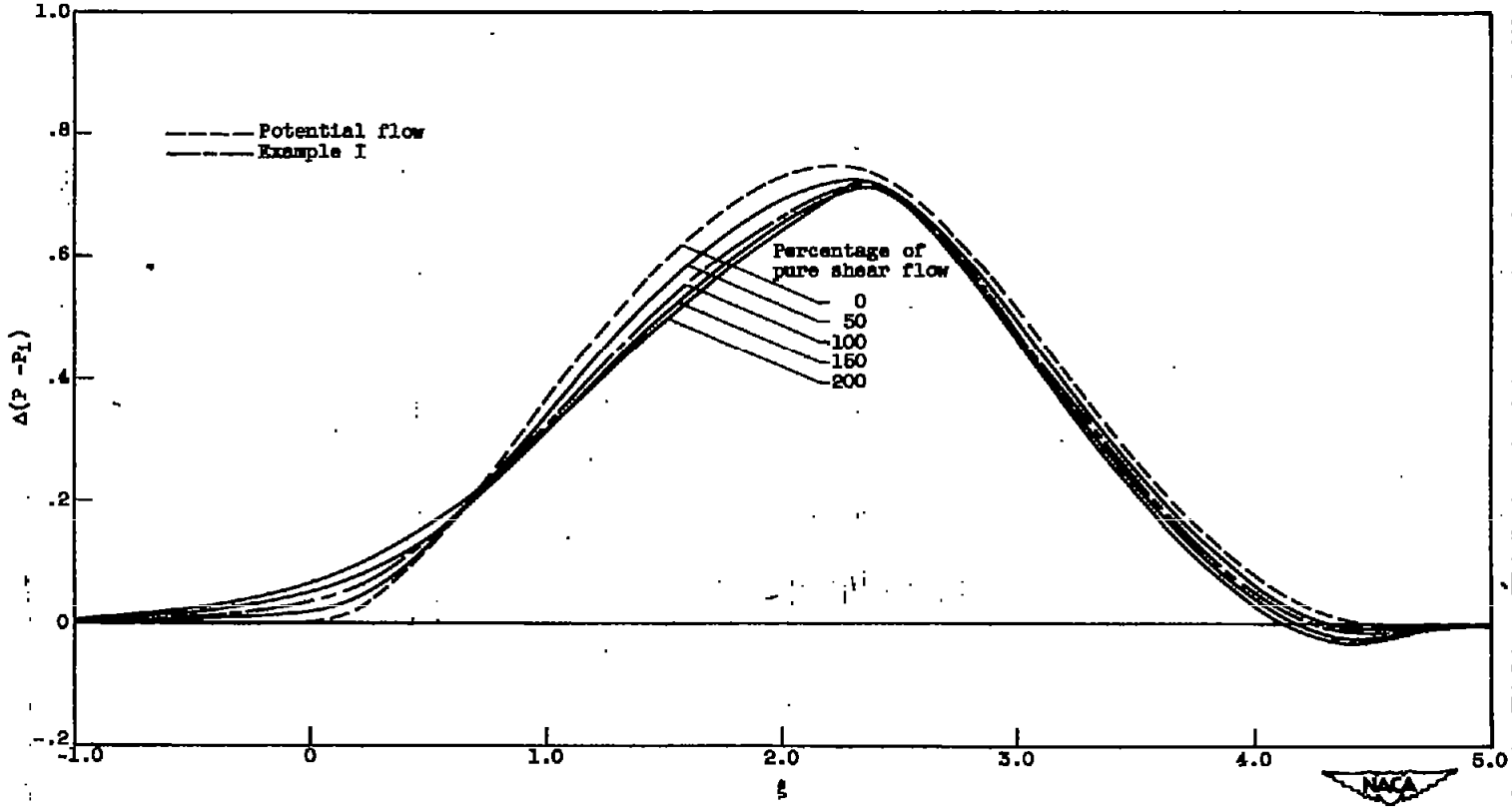

Figure 19. - Difference in pressure coefficient across channel for potential flow plus various percentages of pure shear flow.

NACA-Langley - 8-13-53 - 100